Reciprocal expression of CCAAT/enhancer binding proteins α and ß in hepatoblastomas and its prognostic significance

MINORU TOMIZAWA[1,2], HIROSHI HORIE[3], HIDEKI YAMAMOTO[2], TADASHI MATSUNAGA[3], FUMIAKI SASAKI[3], KOHEI HASHIZUME[3], EISO HIYAMA[3], MICHIO KANEKO[3], SACHIYO SUITA[3], HISAMI ANDO[3], YUTAKA HAYASHI[3], NAOMI OHNUMA[3] and AKIRA NAKAGAWARA[2,3]

[1]Department of Medicine and Clinical Oncology, Chiba University Graduate School of Medicine, 1-8-1 Inohana, Chuo-ku, Chiba City, Chiba 260-8670; [2]Division of Biochemistry, Chiba Cancer Center Research Institute, 666-2 Nitona, Chuo-ku, Chiba City, Chiba 260-8717; [3]The Japanese Study Group for Pediatric Liver Tumor, 1-8-1 Inohana, Chuo-ku, Chiba City, Chiba 260-8670, Japan

Received September 27, 2006; Accepted October 30, 2006

Abstract. Hepatoblastoma is one of the common pediatric solid tumors with frequent mutation of the ß-catenin gene which might be an early event of its carcinogenesis. However, the detailed molecular mechanism is still unknown. We studied the expression levels of CCAAT/enhancer binding protein α (C/EBPα) and C/EBPß, which regulate differentiation and growth of embryonic hepatocytes, to establish whether or not they were involved in affecting the clinical behavior of hepatoblastoma. The quantitative real-time reverse transcriptase-PCR revealed that expression of C/EBPα mRNA was significantly up-regulated in tumors 223% (p=0.013) as compared with that in adjacent normal livers, while expression of C/EBPß was down-regulated to 27% (p=0.002). Of interest, the immunohistochemical analysis showed that expression of C/EBPα was higher and that of C/EBPß lower in the poorly differentiated tumor cells than in the well-differentiated cells within the same tumor. Furthermore, high expression of C/EBPα (p=0.047) as well as low expression of C/EBPß (p=0.025) was significantly associated with poor prognosis of the patients. Cox hazard model suggested that expression of C/EBPα and that of C/EBPß were independent indicators to predict the prognosis from age but not from histology. Thus, expression of C/EBP proteins may play an important role in the genesis and clinical behavior of hepatoblastoma probably by inducing different stages of arrest of differentiation.

Correspondence to: Dr Akira Nakagawara, Division of Biochemistry, Chiba Cancer Center Research Institute, 666-2 Nitona, Chuoh-ku, Chiba 260-8717, Japan
E-mail: akiranak@chiba-cc.jp

Key words: hepatoblast, differentiation, Cox proportional hazard ratio

Introduction

Hepatoblastoma (HBL) is an embryonal tumor and derives from the progenitor cells of the infantile or even the fetal liver which may include hepatoblasts or immature hepatocytes (1). Microscopically, HBL is usually composed of a mixture of well-differentiated tumor cells (fetal type) resembling immature hepatocytes and poorly differentiated cells (embryonal type) similar to embryonic cell components with different proportion (1). Moreover, HBL cells are positive for CK-18 and CK-19, bile duct epithelial markers, as well as α-fetoprotein (AFP), a hepatocyte marker, suggesting that HBL also has the components with a potential to differentiate into both directions (2,3).

Hepatocyte differentiation is controlled by coordinated transcription factors. Both CCAAT/enhancer binding protein (C/EBP)α and C/EBPß are liver-enriched transcription factors, regulating the expression of liver-specific genes. Expression of C/EBPα is observed on day 9.5 of gestation, and C/EBPß on day17.5 in the fetal liver of rodents, suggesting that they may be involved in hepatocyte differentiation (4). The hepatocytes in C/EBPα-deficient mice resemble the embryonal type of HBL cells which may have bipotential ability to differentiate into hepatocytes and bile duct epithelial cells (5). This indicates that C/EBPα may play a role in the growth regulation of HBL cells. C/EBPα is down-regulated while C/EBPß is up-regulated in the remnant liver after partial hepatectomy (6).

We studied expression of C/EBPα and C/EBPß in primary HBLs and found that they were expressed in an opposite manner in HBL and significantly associated with the patient prognosis.

Materials and methods

Tissue samples and RNA isolation. The patients underwent surgical treatment at various hospitals or institutions under the framework of the Japanese Study Group for Pediatric Liver Tumor (JPLT) between 1991 and 2005. The extent of the disease (stage) was classified according to that of SIOPEL

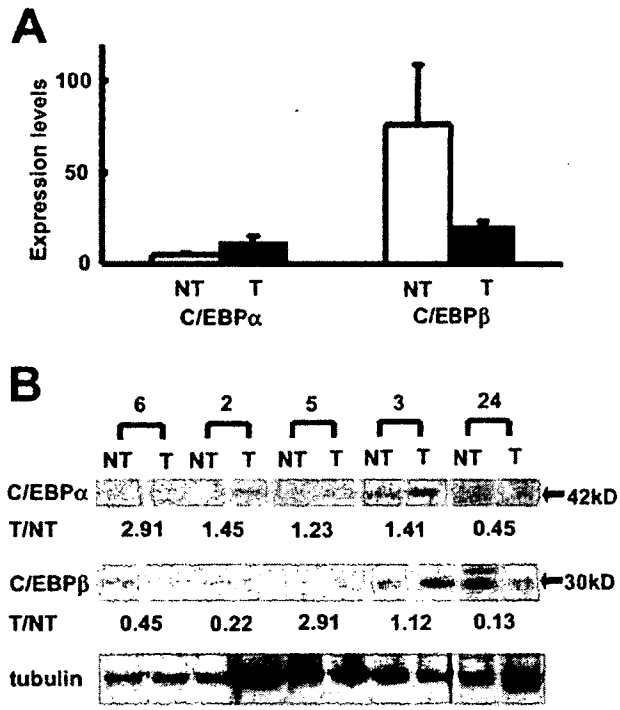

Figure 1. Real-time quantitiative PCR and Western blot analysis of hepatoblastoma with C/EBPα and C/EBPß. (A) Expression levels of C/EBPα and C/EBPß were analyzed with real-time quantitative PCR (x1000) (mean ± standard error). NT, non-tumorous tissue; T, tumorous tissue; n=24. (B) Western blot analysis was performed with representative patients (patient numbers; 6, 2, 5, 3 and 24). The intensities of C/EBPα (42 kD) and C/EBPß (30 kD) proteins expression were normalized against α-tubulin, and the ratio of T to NT was calculated. T/NT, a ratio of the C/EBP expression level in tumorous tissue divided by that in non-tumorous tissue.

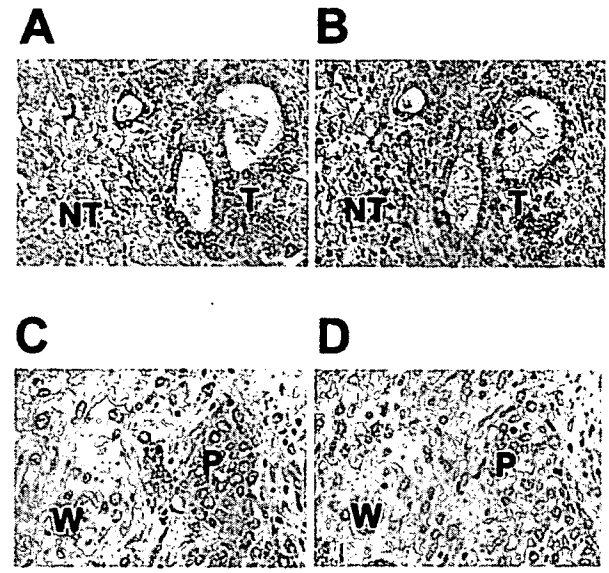

Figure 2. Immunohistochemistry of C/EBPα and C/EBPß in hepatoblastomas. Surgical specimens were immunohistochemically stained with anti-C/EBPα or -C/EBPß antibody. (A) C/EBPα was weakly positive in the cytoplasm and nuclei of normal hepatocytes in non-tumorous tissues (NT). C/EBPα was strongly positive in the cytoplasm and the nuclei of tumor cells (T). (B) C/EBPß was strongly positive in the cytoplasm and nuclei of hepatocytes (NT). C/EBPß was weakly positive in the cytoplasm of tumor cells. (T) (C) C/EBPα was more strongly positive in the cytoplasm of poorly differentiated tumor cells (P) than in that of well differentiated tumor cells (W). (D) C/EBPß was more weakly positive in the cytoplasm of poorly differentiated tumor cells (P) than in that of well differentiated tumor cells (W). Original magnification: x100 (A and B), x400 (C and D).

(7). Histopathology of HBL was according to the classification by the Japanese Society of Pathology which includes well differentiated (fetal) and poorly differentiated (embryonal) types. With informed consent, tumor tissues and their corresponding normal liver tissues were obtained at surgery, immediately frozen, and stored at -80°C until use. Frozen tumor tissues were obtained from 46 patients with HBL, and corresponding normal liver tissues were available from the rejected tissues of 24 patients. All specimens used in this study were provided by the Tissue Bank of JPLT. The JPLT Review Board as well as the Chiba Cancer Center institutional committee approved the analysis with the specimens. Total RNA was prepared by the conventional guanidine thiocyanate-phenol-chloroform procedure.

Real-time quantitative PCR. First-strand cDNA was prepared with 5 μg of total RNA from the surgical specimens, with 200 units of Superscript II reverse transcriptase (Invitrogen Corp., Carlsbad, CA), and 160 pmol of random primers (Takara, Ohtsu, Japan). Synthesized cDNA was subjected to a quantitative real-time PCR (PE Biosystems, Foster City, CA) (8). The primers for C/EBPα were 5'-CGGACTTGG TGCGTCTAAG-3' for 5', 5'-GAGGCAGGAAACCTCC AAAT-3' for 3', and 5'-GAGGCAGGAAACCTCCAAAT-3' for the detection probe; the primers for C/EBPß were 5'-AG CGCGGCGACGAGTACAAGATC-3' for 5', 5'-ACCTTGT GCTGCGTCTCCA-3' for 3', and 5'-CGCGAGCGCAACA ACATCGC-3' for the detection probe. Taq-Man ß-actin control reagents (Perkin Elmer Inc., Wellesley, MA) were used for the amplification of ß-actin as recommended by the manufacturer.

Immunohistochemistry and Western blot analysis. Nine HBL tissues were used for immunohistochemistry, and 5 paired (HBL tissue and its adjacent normal tissue) samples were used for Western blot analysis. Primary antibodies were polyclonal rabbit anti-rat C/EBPα (1:100 dilution, Santa Cruz Biotechnology Inc., Santa Cruz, CA), polyclonal rabbit anti-rat C/EBPß (1:100, dilution, Santa Cruz Biotechnology Inc.), and mouse monoclonal anti-α-tubulin antibody (Lab Vision, Fremont, CA). The exposed films from Western blot analysis were scanned, and the images were analyzed with the software program ImageJ 1.34s (NIH, Bethesda, MD).

Statistical analysis. Kaplan-Meier survival curves were calculated, and survival distributions were compared using the log-rank test. Proportional Cox regression models were used to explore associations among C/EBPα, C/EBPß, age, stage, alpha-feto protein, pathology, and survival. Statistical significance was declared at P-value <0.05. Statistical analysis was performed using Stata 7.0 (Stata Corp., College Station, TX).

Results

The expression levels of C/EBPα and C/EBPß mRNA were measured in primary HBLs and their adjacent normal liver tissues by using quantitative real-time RT-PCR (Fig. 1A).

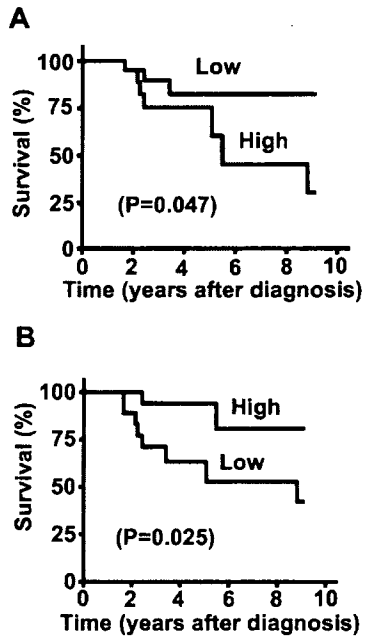

Figure 3. Kaplan-Meier survival curves for patients with hepatoblastoma. Survival of patients with hepatoblastoma after surgery was analyzed (Kaplan-Meier). Patients were divided into two groups for each factor. Patients with higher expression levels of C/EBPα than the median (A) (P=0.047), and lower expression levels of C/EBPß than the median (B) (P=0.025) were associated with shorter survival. P-value for log-rank test is shown in parentheses; n=46.

Table I. Proportional Cox regression models using C/EBPα and C/EBPß and dichotomous factors of age and pathology.

Model	Factor	HR (95% C.I.)	P-value
A	C/EBPα	3.57 (0.91-14.0)	0.068
B	C/EBPß	0.20 (0.04-0.96)	0.044
C	Age	0.27 (0.07-1.02)	0.054
D	Pathology	13.5 (1.70-107)	0.014
E	C/EBPα	4.14 (1.04-16.5)	0.044
	C/EBPß	0.18 (0.04-0.86)	0.031
F	C/EBPα	5.66 (1.32-24.2)	0.019
	C/EBPß	0.17 (0.04-0.81)	0.027
	Age	0.15 (0.03-0.76)	0.022
G	C/EBPα	2.30 (0.56-9.41)	0.25
	C/EBPß	0.40 (0.08-2.07)	0.28
	Pathology	7.95 (0.87-72.6)	0.066

HR, hazard ratio showing the relative risk of death of the first category relative to the second; parenthesis, 95% confidence interval (C.I.); C/EBPα and C/EBPß, high vs. low expression levels of C/EBPα and C/EBPß in tumor with real-time quantitative PCR; n=46.

The C/EBPα expression was significantly high in the tumors (mean ± SEM: 11.6±3.2, n=24) as compared with that in the normal livers (5.1±0.9, n=24; p=0.013). On the other hand, the expression of C/EBPß was significantly lower in HBL tissues (20.4±2.7, n=24) than that in the normal liver tissues (75.8±33, n=24; p=0.002). To confirm these results, we next measured expression levels of C/EBPα and C/EBPß proteins in 5 paired samples of tumor and its corresponding normal liver by Western blot analysis. The data obtained showed a tendency of up-regulation of C/EBPα and down-regulation of C/EBPß in the tumor tissues as compared with the paired normal livers (Fig. 1B).

Fig. 2 shows immunohistochemical stainings of primary HBLs. C/EBPα was weakly positive in the cytoplasm and nuclei of normal hepatocytes, and strongly positive mainly in the cytoplasm of tumor cells (Fig. 2A). By contrast, C/EBPß was rather positive in the cytoplasm and nuclei of hepatocytes in the adjacent normal livers, whereas it was weakly positive in the cytoplasm of the tumor cells (Fig. 2B). In the same tumor tissues, C/EBPα was more strongly positive in the poorly differentiated tumor cells than the adjacent well-differentiated tumor cells (Fig. 2C). C/EBPß was weakly positive in the poorly differentiated tumor cells, whereas it was almost negative in the well-differentiated tumor cells (Fig. 2D).

The Kaplan-Meier cumulative survival curves are shown in Fig. 3. The high levels of expression of C/EBPα mRNA were significantly associated with poor patient survival (68.2% 5-year survival rate, n=22, vs. 87.5%, n=24; p=0.047), whereas high levels of expression of C/EBPß mRNA were significantly correlated with favorable prognosis (92.6% 5-year survival rate, n=27, vs. 57.9%, n=19; p=0.025). Univariate Cox regression analysis of 46 patients with HBL showed that expression of C/EBPß (high vs. low expression; p=0.044), age (<1-year vs. ≥1-year; p=0.054) and histopathology (well vs. poorly differentiated; p=0.014) were significant indicators of the prognosis, while expression of C/EBPα (p=0.068) was marginally significant as a prognostic factor of HBLs (Table I). Multivariate analysis using Cox model showed that C/EBPα and C/EBPß were significantly related to survival in a model jointly with each factor (P<0.05, model E). C/EBPα and C/EBPß were significantly related to survival (P<0.047) even after controlling age (P=0.022, model F). Finally, since 9 out of 10 deceased patients had poorly differentiated histopathology, C/EBPα and C/EBPß would lose significance in a model including pathology (model G).

Discussion

The basic studies of hepatoblastoma have recently provided important information to understanding of genesis and progression of HBL. The ß-catenin gene was discovered to be mutated and translocated into the cellular nucleus (9). However, high frequency of aberration of the Wnt signaling appeared to be an early event and the ß-*catenin* mutation itself did not have prognostic significance (8). The studies using comparative genomic hybridization (CGH) presented an interesting pattern of the chromosomal aberrations in HBLs (10). The comprehensive cDNA project of HBLs has also given some insights into the understanding of the molecular aspect of HBLs by identifying a large number of

differentially expressed genes between the HBL tumors and their corresponding normal livers, that indentified Plk1 as a highly expressed gene in HBLs (11). However, expression of most of the genes was not predictive for prognosis.

The C/EBPα gene is mapped to chromosome 19q, which is often gained in HBLs and has been found to be up-regulated in HBLs (12). However, the gene is mutated in acute myeloid leukemia and is often down-regulated in some other cancers, suggesting that C/EBPα may function as a tumor suppressor (13,14). In addition, our previous study suggested that both C/EBPα and C/EBPß were down-regulated in hepatocellular carcinomas as compared with the adjacent non-tumorous liver tissues (15). These suggest that C/EBPα may play a different role in HBLs from other cancers.

C/EBPß was down-regulated in HBLs as compared with the corresponding normal livers and correlated with poor prognosis in the HBL patients, that was similar to HCC and other cancers (15,16). Buck *et al* reported that overexpression of C/EBPß in HepG2 cells, a human HCC cell line, suppressed proliferation of the cells (17). Therefore, C/EBPß might function as a tumor suppressor in HBL cells. In addition, C/EBPß may also play a role in regulating differentiation of HBL cells because the gene is expressed in mature hepatocytes and is reported to be indispensable for induction of the lever-specific genes.

Thus, both C/EBPα and C/EBPß may play important roles in regulating growth and differentiation of HBLs. Moreover, a small amount of tumor biopsy samples could be used for measuring the mRNA expression levels of both genes for predicting aggressiveness of the HBL tumors.

Acknowledgements

This study was supported by the Japan Society for the Promotion of Science (JSPS), the Ministry of Education, Science, Sports, and Culture, and the Ministry of Health, Labour, and Welfare. We thank Dr Hajime Takayasu, Dr Shin-ichi Yamada, and Dr Miki Ohira for their advice.

References

1. Ishak KG and Glunz PR: Hepatoblastoma and hepatocarcinoma in infancy and childhood. Report of 47 cases. Cancer 20: 396-422, 1967.
2. Pietsch T, Fonatsch C, Albrecht S, Maschek H, Wolf HK and von Schweinitz D: Characterization of the continuous cell line HepT1 derived from a human hepatoblastoma. Lab Invest 74: 809-818, 1996.
3. Ruck P, Xiao JC and Kaiserling E: Small epithelial cells and the histogenesis of hepatoblastoma. Electron microscopic, immunoelectron microscopic, and immunohistochemical findings. Am J Pathol 148: 321-329, 1996.
4. Shiojiri N, Takeshita K, Yamasaki H and Iwata T: Suppression of C/EBP alpha expression in biliary cell differentiation from hepatoblasts during mouse liver development. J Hepatol 41: 790-798, 2004.
5. Tomizawa M, Garfield S, Factor V and Xanthopoulos KG: Hepatocytes deficient in CCAAT/enhancer binding protein alpha (C/EBP alpha) exhibit both hepatocyte and biliary epithelial cell character. Biochem Biophys Res Commun 249: 1-5, 1998.
6. Flodby P, Antonson P, Barlow C, Blanck A, Porsch-Hallstrom I and Xanthopoulos KG: Differential patterns of expression of three C/EBP isoforms, HNF-1, and HNF-4 after partial hepatectomy in rats. Exp Cell Res 208: 248-256, 1993.
7. Perilongo G, Shafford E and Plaschkes J: SIOPEL trials using preoperative chemotherapy in hepatoblastoma. Lancet Oncol 1: 94-100, 2000.
8. Takayasu H, Horie H, Hiyama E, *et al*: Frequent deletions and mutations of the beta-catenin gene are associated with overexpression of cyclin D1 and fibronectin and poorly differentiated histology in childhood hepatoblastoma. Clin Cancer Res 7: 901-908, 2001.
9. Park WS, Oh RR, Park JY, *et al*: Nuclear localization of beta-catenin is an important prognostic factor in hepatoblastoma. J Pathol 193: 483-490, 2001.
10. Weber RG, Pietsch T, von Schweinitz D and Lichter P: Characterization of genomic alterations in hepatoblastomas. A role for gains on chromosomes 8q and 20 as predictors of poor outcome. Am J Pathol 157: 571-578, 2000.
11. Yamada S, Ohira M, Horie H, *et al*: Expression profiling and differential screening between hepatoblastomas and the corresponding normal livers: identification of high expression of the PLK1 oncogene as a poor-prognostic indicator of hepatoblastomas. Oncogene 23: 5901-5911, 2004.
12. Gray SG, Kytola S, Matsunaga T, Larsson C and Ekstrom TJ: Comparative genomic hybridization reveals population-based genetic alterations in hepatoblastomas. Br J Cancer 83: 1020-1025, 2000.
13. Pabst T, Mueller BU, Zhang P, *et al*: Dominant-negative mutations of CEBPA, encoding CCAAT/enhancer binding protein-alpha (C/EBPalpha), in acute myeloid leukemia. Nat Genet 27: 263-270, 2001.
14. Halmos B, Huettner CS, Kocher O, Ferenczi K, Karp DD and Tenen DG: Down-regulation and antiproliferative role of C/EBPalpha in lung cancer. Cancer Res 62: 528-534, 2002.
15. Tomizawa M, Watanabe K, Saisho H, Nakagawara A and Tagawa M: Down-regulated expression of the CCAAT/enhancer binding protein alpha and beta genes in human hepatocellular carcinoma: a possible prognostic marker. Anticancer Res 23: 351-354, 2003.
16. Oh HS and Smart RC: Expression of CCAAT/enhancer binding proteins (C/EBP) is associated with squamous differentiation in epidermis and isolated primary keratinocytes and is altered in skin neoplasms. J Invest Dermatol 110: 939-945, 1998.
17. Buck M, Turler H and Chojkier M: LAP (NF-IL-6), a tissue-specific transcriptional activator, is an inhibitor of hepatoma cell proliferation. EMBO J 13: 851-860, 1994.

J Cancer Res Clin Oncol (2007) 133:185–192
DOI 10.1007/s00432-006-0156-y

ORIGINAL PAPER

Relationship of *DDX1* and *NAG* gene amplification/ overexpression to the prognosis of patients with *MYCN*-amplified neuroblastoma

Setsuko Kaneko · Miki Ohira · Yohko Nakamura · Eriko Isogai · Akira Nakagawara · Michio Kaneko

Received: 14 June 2006 / Accepted: 28 August 2006 / Published online: 7 October 2006

Abstract
Purpose Amplification of the *MYCN* gene strongly correlates with advanced stage, rapid tumor progression and poor prognosis in neuroblastoma (NB). Several genes in the *MYCN* amplicon, including the DEAD box polypeptide 1 (*DDX1*) gene, and neuroblastoma-amplified gene (*NAG* gene), have been found to be frequently co-amplified with *MYCN* in NB. The aim of this study was to clarify the prognostic significance of the co-amplification or overexpression of *DDX1* and *NAG* with *MYCN*.
Procedure The gene copy numbers and mRNA expression levels of *MYCN*, *DDX1*, and *NAG* in 113 primary NBs were determined by the real-time quantitative polymerase chain reaction or quantitative reverse transcriptase/polymerase chain reaction assay. The relationships between gene co-amplification/overexpression status and stage, age at diagnosis, and overall survival were analyzed.
Results For evaluating the frequency of *DDX1* and *NAG* co-amplification, it proved appropriate to discriminate NBs with <40 copies of *MYCN* amplification from those with ≥40 copies of *MYCN* (*DDX1*, $p = 0.00058$; *NAG*, $p = 0.0242$, χ^2 for independence test). In patients with *MYCN*-amplified NB aged ≥18 months, those with tumor with enhanced *DDX1* expression and low-*NAG* expression showed a significantly better outcome than those with low-*DDX1* expression or enhanced *NAG* expression ($p = 0.0245$, log-rank test). None of the gene expression statuses had a significant relation to disease stage or survival for patients <18 months old. No relationship between any gene co-amplification status and disease stage, age at diagnosis, or overall survival was found.
Conclusions Our findings suggest that there may be a subset of NB in which enhanced *DDX1* and low-*NAG* expression consequent to *DDX1* co-amplification without *NAG* amplification contributes to susceptibility to intensive therapy. A larger study using an age cut-off of 18 months will be required.

Keywords Neuroblastoma · *MYCN* · *DDX1* · *NAG*

Abbreviations

NB	Neuroblastoma
DDX1	DEAD box polypeptide 1 gene
NAG	Neuroblastoma-amplified gene
hnRNP K	Heterogeneous nuclear ribonucleoprotein K
q-PCR	Quantitative polymerase chain reaction
q-RT-PCR	Quantitative reverse transcriptase/ polymerase chain reaction
BCM	B-cell maturation factor gene
GAPDH	Glyceraldehyde 3-phosphate dehydrogenase

S. Kaneko (✉) · M. Kaneko
Department of Pediatric Surgery,
Institute of Clinical Medicine,
University of Tsukuba,
Ibaraki 305-8575, Japan
e-mail: mkaneko@md.tsukuba.ac.jp

M. Ohira · Y. Nakamura · E. Isogai · A. Nakagawara
Division of Biochemistry,
Chiba Cancer Center Research Institute,
Chiba 260-8717, Japan

Introduction

Neuroblastoma (NB) is one of the most common malignant solid tumors in childhood. It presents with

wide aggression from spontaneous regression or tumor maturation to rapid progression and fatality in most metastatic tumors diagnosed in children more than 1 year old. *MYCN* amplification occurs in about 25% of NB and is one of the most important markers in determining the aggressiveness of NB. Amplification of *MYCN* strongly correlates with advanced disease stage, rapid tumor progression and poor prognosis (Brodeur et al. 1984; Seeger et al. 1985; Brodeur and Seeger 1986). The size of the *MYCN* amplicon can span from 100 to 1,500 kb (Amler and Schwab 1989). Consequently, it is possible to suggest that additional genes being present in the amplicon and co-amplified with *MYCN* may contribute to the tumor phenotype. So far, several genes including the *DDX1* (DEAD box polypeptide 1) gene and *NAG* (NB-amplified gene) gene have been found to be frequently co-amplified with *MYCN* in NB (Beheshti et al. 2003; Scott et al. 2003a).

The *DDX1* is one of a family of genes that encode DEAD (asp-glu-ala-asp) box proteins. This gene maps to chromosome band 2p24 and 340 kb 5′ of *MYCN* (Godbout and Squire 1993; Kuroda et al. 1996). Proteins with the DEAD box motif are putative ATP-dependent RNA helicases and more than 30 proteins have been identified from bacteria to humans (De Valoir et al. 1991; Kitajima et al. 1994). By altering the RNA secondary structure, they are implicated in diverse cellular processes such as RNA splicing, ribosome assembly, and translation initiation (Tanner and Linder 2001). Some members of the family are differentially expressed during embryogenesis, cellular growth, and division (Schmid and Linder 1992; Iost and Dreyfus 1994; Godbout et al. 2002). The biological function of DDX1 remains unknown. In recent studies, DDX1 was found to associate with factors involved in 3′-end cleavage and polyadenylation of pre-mRNAs (Bleoo et al. 2001). DDX1 was also shown to have protein–protein interaction with heterogeneous nuclear ribonucleoprotein K (hnRNP K), and to have poly(A) RNA binding activity (Chen et al. 2002).

The *DDX1* gene has been known to be co-amplified with *MYCN* in 40–70% of NBs. There are reports showing a trend toward a worse clinical outcome with *MYCN* and *DDX1* co-amplification (Squire et al. 1995; George et al. 1997). Others have reported no significant difference in the clinical outcome or survival between patients with or without *DDX1* co-amplification (Manohar et al. 1995; De Preter et al. 2002). In a recent study of 98 *MYCN*-amplified NBs, a significant correlation of *DDX1* co-amplification with a better prognosis and improved patient survival was shown by using semiquantitative multiplex PCR (Weber et al. 2004). In contrast to the observations by Weber et al., De Preter et al. have concluded that *DDX1* co-amplification had no significant prognostic value in *MYCN*-amplified tumors by re-evaluating their data (De Preter et al. 2005). The prognostic significance of *MYCN* and *DDX1* co-amplification has not been determined.

Recently, Scott et al. reported that the 5′end of *NAG* is located 30 kb telomeric to *DDX1*, with the two genes lying in opposite orientations (Scott et al. 2003b). They found a significant association between low-disease stage in *MYCN*-amplified tumors and *NAG* co-amplification. The function of NAG is as yet unclear.

To date, there have been no reports of measuring and analyzing accurate copy numbers and precise mRNA expression levels of *MYCN*, *DDX1*, and *NAG* genes in NB. In order to clarify the prognostic significance of the co-amplification or gene expression of *DDX1* and *NAG* with *MYCN*, we determined gene copy numbers and mRNA expression levels of *MYCN*, *DDX1*, and *NAG* genes in 113 primary NBs using the real-time quantitative polymerase chain reaction (q-PCR) or quantitative reverse transcriptase/polymerase chain reaction (q-RT-PCR) assay. The results were analyzed in relation to stage, age at diagnosis and overall survival.

Materials and methods

Tumor samples

One hundred and thirteen primary NBs were obtained from the Department of Pediatric Surgery, University of Tsukuba, and the Division of Biochemistry, Chiba Cancer Center Research Institute, Japan. Tumors detected by mass screening were excluded. Patients were aged between 0 months and 14 years at diagnosis (median 18 months). All 52 nonsurvivors died of progressive disease, while 59 of 61 survivors are free of the disease.

Tumors with the haploid *MYCN* gene copy number of more than five and less than two by the q-PCR assay were considered as *MYCN* amplified and unamplified, respectively.

DNA or RNA extraction

Tumor DNA was isolated by proteinase K/SDS digestion followed by phenol–chloroform extraction according to the standard protocol. DNA from human

placenta and a NB cell line CHP 134 were used as templates for the reference B-cell maturation factor (*BCM*) gene and test genes, respectively. The CHP 134 cell was found to have multiple copies of *MYCN*, *DDX1*, and *NAG* genes by preliminary q-PCR.

Total RNA was prepared from frozen tumor tissue according to the Acid Guanidinium–Phenol–Chloroform method (Chomczynski and Sacchi 1987). One microgram of each RNA was incubated with random primers and Superscript II reverse transcriptase (Invitrogen, Carlsbad, CA, USA) to yield cDNA.

Real-time q-PCR

Real-time q-PCR was carried out using the ABI Prism 7700 Sequence Detection System (Applied Biosystems, Foster City, CA, USA) as described by De Preter et al. with modification (De Preter et al. 2002). For quantification of the gene copy number, TaqMan probe assay was performed. The nucleotide sequences of the primers used are *MYCN*-f 5′-CGCAAAAGCC ACCTCTCATTA-3′ and *MYCN*-r 5′-TCCAGCAG ATGCCACATAAGG-3′, *DDX1*-f 5′-TAGGAGGAG GTGATGTACTTATGGTAA-3′ and *DDX1*-r 5′-AG CCTATGCAATTCTTAGAGTGTGT-3′, *NAG*-f 5′G ACCAAGAACTTCTTTCCCTGC-3′ and *NAG*-r 5′-GGTCAACAATACGTGGATAGAAGG-3′, and *BCM*-f 5′-CGACTCTGACCATTGCTTTCC-3′ and *BCM*-r 5′-AAGCAGCTGGCAGGCTCTT-3′.

The sequences of the TaqMan probes are *MYCN* 5′-FAM-TTCTGTAAATACCATTGACACATCCG CCTT-TAMRA-3′, *DDX1* 5′-FAM-CCCAGCTACC AATCACCTCACCAAATT-TAMRA-3′, *NAG* 5′-F AM-CAAGCTGCTGGTGAAGTGTGTCTCCA-T AMRA-3′ and *BCM* 5′-FAM-CAACCATTCTTGTC ACCACGAAAACGAA-TAMRA-3′. Twenty microliter of PCR reaction mixture for copy number determination consisted of template DNA, 1× q-PCR Mastermix (EUROGENTEC, Liege, Belgium), 300 nM of each primer and 200 nM of TaqMan probe. *MYCN*, *DDX1* or *NAG* gene assay was performed containing no-template control, standard CHP 134 DNA of five serial tenfold dilutions ranging from 100 ng to 10 pg, 10 ng of human placental DNA as a calibrator and ~10 ng of tumor DNA. The reference *BCM* gene assay included no-template control, standard human placental DNA of four serial tenfold dilutions ranging from 200 to 0.2 ng, 10 ng of human placental DNA as a calibrator and ~10 ng of tumor DNA. *BCM* gene is mapped to 16p13.1 and is located in a chromosomal region that rarely shows genetic abnormality (Vandesompele et al. 2001). Experiments were carried out in triplicate. The thermal cycling conditions for q-PCR and q-RT-PCR were: 50°C for 2 min, 95°C for 10 min, 45 cycles at 95°C for 15 s and 60°C for 1 min.

Real-time q-RT-PCR

Expression levels of *MYCN*, *DDX1*, and *NAG* genes were measured in cDNA by the ABI Prism 7700 Sequence Detection System (Applied Biosystems). Human glyceraldehyde 3-phosphate dehydrogenase (*GAPDH*) was used as an internal control gene. cDNA from one of the 113 samples examined was used as the standard template because of its appropriate expression levels of *MYCN*, *DDX1*, *NAG*, and *GAPDH* mRNA by preliminary q-RT-PCR. The specific primers used are *MYCN*-f 5′-CACAAGGCCCTCAGTA CCTC-3′ and *MYCN*-r 5′- CAGTGACCACGTCGA TTTCTT-3′, *DDX1*-f 5′-TGGAAGAGATGGATT GGCTC-3′ and *DDX1*-r 5′-CCTGTTTCTGCAGCC ATAAGTAC-3′, *NAG*-f 5′-CAAATCACGGCAGT CACTACG-3′ and *NAG*-r 5′-ACACACTTCACCA GCAGCTTG-3′, and *GAPDH*-f 5′-GAAGGTGAA GGTCGGAGTC-3′ and *GAPDH*-r 5′-GAAGATGG TGATGGGATTTC-3′. The sequences of the TaqMan probes are *MYCN* 5′-FAM-AGAGGACACCCTGA GCGATTCAGATG-TAMRA-3′, *DDX1* 5′-FAM-C CAACTGATATCCAGGCTGAATCTATCCCA-T AMRA-3′, *NAG* 5′-FAM-TGTGACCAAGAACTTC TTTCCCTGCTCCT-TAMRA-3′ and *GAPDH* 5′-F AM-CAAGCTTCCCGTTCTCAGCC-TAMRA-3′. The primers and probes were designed to be located on exons 2–3 for *MYCN* mRNA, exons 2–4 for *DDX1* mRNA, exons 51–52 for *NAG* mRNA, and exons 4–6 for *GAPDH* mRNA.

Twenty microliter of the PCR reaction mixture for quantification contained template cDNA, 1× qPCR Mastermix (EUROGENTEC), 300 nM of each primer and 200 nM of TaqMan probe. Each assay consisted of no-template control, standard cDNA of five serial tenfold dilutions ranging from 1 μg to 0.1 ng, and ~5 ng of tumor cDNA.

Statistical analysis

The relation of *DDX1* or *NAG* gene amplification to *MYCN* gene copy number was tested using χ^2 for an independence test. Correlations between the gene amplification/expression status and disease stage or age at diagnosis were compared by χ^2 for an independence test or Fisher's exact probability test. Mann–Whitney's *U*-test was used to evaluate the relationship between the gene expression level in tumors with or without gene amplification. Survival analysis was performed according to the Kaplan–Meier method and the log-rank test.

Results

The haploid *MYCN*, *DDX1*, and *NAG* gene copy number

Seventy-two of 113 tumors examined had *MYCN* amplification. Forty-one tumors were *MYCN*-unamplified; 17 in stages 1, 2 or 4S, nine in stage 3, and 15 in stage 4. Twenty-five and 16 patients were aged <18 and ≥18 months at diagnosis, respectively. Seven of 41 patients died of disease, while all 34 survivors are free of disease. Patients with *MYCN*-amplified NB included four with stage 1, two with stage 2, two with stage 4s, 12 with stage 3, and 52 patients with stage 4 disease. Of 72 patients with *MYCN*-amplified tumor, 45 patients died of disease, while 25 of 27 survivors are free of disease. The follow-up period for *MYCN*-amplified survivors ranged from 17 to 93 months.

In 72 *MYCN*-amplified NBs, *DDX1*, and *NAG* genes were found to be co-amplified in 49 (68.1%) and 19 (26.4%) tumors, respectively (Fig. 1a, b). All 19 tumors with *NAG* amplification had also *DDX1* amplification. Forty-one tumors without *MYCN* amplification were unamplified for *DDX1* and *NAG*. By plotting precise gene copy numbers of *MYCN* and *DDX1*, and *MYCN* and *NAG* of each tumor on the same graphs, we found for the first time that NB with lower copies of *MYCN* amplification tended to a more frequent *DDX1* and *NAG* co-amplification than those with higher copies of *MYCN*. For evaluating the frequency of *DDX1* and *NAG* co-amplification, it proved appropriate to discriminate NBs with <40 copies of *MYCN* amplification from those with ≥40 copies of *MYCN* (*DDX1*, $p = 0.00058$; *NAG*, $p = 0.0242$, χ^2 for independence test) (Fig. 1a, b).

Overall survival of patients with *MYCN*-amplified NB with or without *DDX1* and *NAG* co-amplification

For the 72 patients with *MYCN*-amplified NB, no statistically significant difference in survival probability was found among three gene co-amplification statuses, patients with tumor with *MYCN* amplification alone (*MYCN* alone), those with *DDX1* co-amplification alone (*MYCN* + *DDX1*), and those with both *DDX1* and *NAG* co-amplification (*MYCN* + *DDX1* + *NAG*) (*MYCN* alone versus *MYCN* + *DDX1*, $p = 0.465$; *MYCN* alone versus *MYCN* + *DDX1* + *NAG*, $p = 0.719$; *MYCN* + *DDX1* versus *MYCN* + *DDX1* + *NAG*, $p = 0.148$, log-rank test) (Fig. 2). We found no significant difference in overall survival between patients with tumor with *MYCN* amplification alone and those with *DDX1*-co-amplified NB regardless of *NAG* co-amplification ($p = 0.763$, log-rank test).

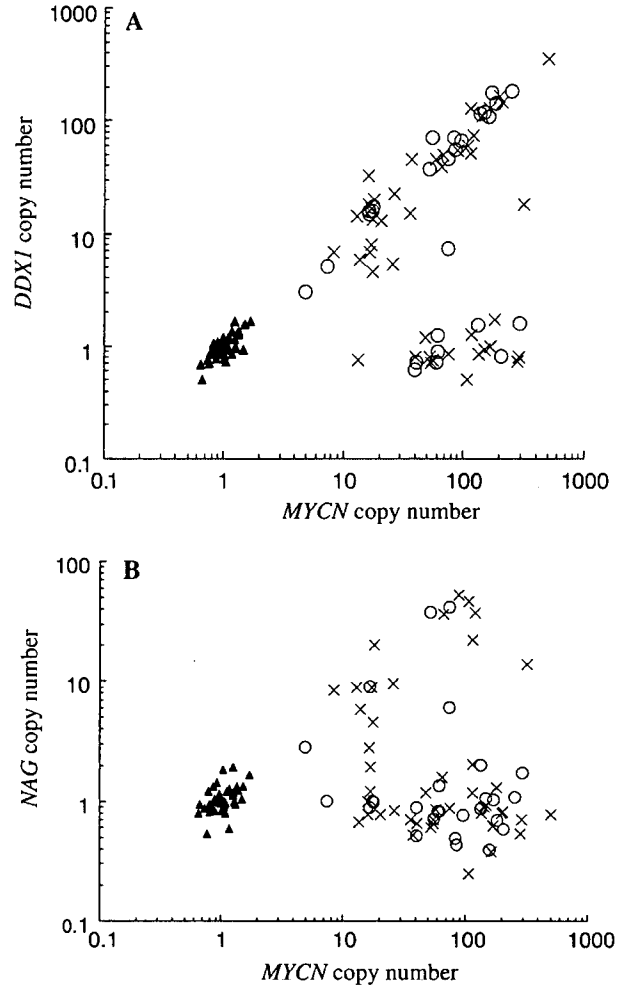

Fig. 1 The haploid *MYCN* and *DDX1* gene copy numbers (**a**), and *MYCN* and *NAG* gene copy numbers (**b**) in 113 NBs were determined by real-time q-PCR. *Open circle*, survivors with *MYCN* amplification ($n = 27$); *cross*, nonsurvivors with *MYCN* amplification ($n = 45$); *filled triangle*, patients without *MYCN* amplification ($n = 41$)

Relation of gene co-amplification status to disease stage or age at diagnosis

Table 1 shows the gene co-amplification status, disease stage and age at diagnosis of 72 patients with *MYCN*-amplified NB. Recently, an age cut-off higher than 12 months has been proposed as a prognostic predictor for comparison of survival rate in NB, suggesting an appropriate age cut-off of 18 months (London et al. 2005).

None of the gene co-amplification statuses had a significant correlation with disease stage (stages 1, 2, 3, and 4s versus stage 4) or age at diagnosis (<18 months versus ≥18 months) (data not shown), with the exception of *NAG*, which tended toward a more frequent co-amplification with *MYCN* in stage 4 (17/52, 32.7%)

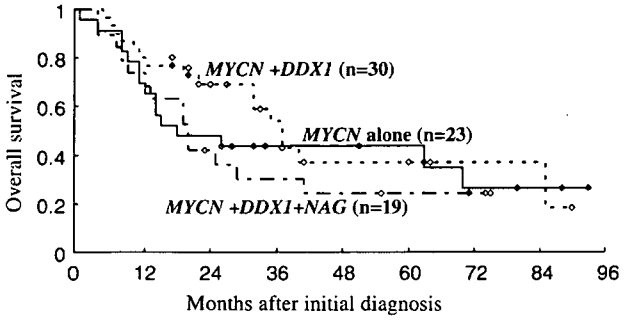

Fig. 2 Overall survival for patients with *MYCN*-amplified NB with or without *DDX1* and *NAG* co-amplification. No statistically significant difference in survival probability was found among three gene co-amplification statuses (*MYCN* alone versus *MYCN* + *DDX1*, $p = 0.465$; *MYCN* alone versus *MYCN* + *DDX1* + *NAG*, $p = 0.719$; *MYCN* + *DDX1* versus *MYCN* + *DDX1* + *NAG*, $p = 0.148$, log-rank test)

Table 1 Gene co-amplification status, disease stage and age at diagnosis of 72 patients with *MYCN*-amplified NB. There was no significant correlation between any gene co-amplification status and disease stage (stages 1, 2, 3, and 4s versus stage 4) or age at diagnosis among 72 patients with *MYCN*-amplified NB, with the exception of *NAG*, which tended toward a more frequent co-amplification with *MYCN* in stage 4 compared with stages 1, 2, 3, and 4s ($p = 0.0504$, χ^2 for independence test)

	Stage			Age (months)	
	1, 2 and 4s	3	4	<18	≥18
MYCN alone	4	4	15	10	13
MYCN+DDX1	4	6	20	11	19
MYCN+ DDX1+NAG	0	2	17	10	9
Total	8	12	52	31	41

compared with stages 1, 2, 3, and 4s (2/20, 10.0%) ($p = 0.0504$, χ^2 for independence test).

The expression level of *MYCN*, *DDX1*, and *NAG*

We determined the precise expression levels of *MYCN*, *DDX1*, and *NAG* in 108 of 113 NBs. Sixty-seven of 108 tumors had *MYCN* amplification. The *MYCN*-amplified tumors had a significantly higher expression level of *MYCN* compared with *MYCN*-unamplified tumors ($p = 8.22 \times 10^{-15}$, Mann–Whitney's *U*-test). None of the *MYCN*-unamplified tumors showed an overexpression of *MYCN*, *DDX1*, and *NAG* (data not shown). We classified *DDX1* or *NAG* gene expression levels higher than the highest in *MYCN*-unamplified tumors as enhanced.

In general, *DDX1* expression increased according to the *DDX1* copy number (Fig. 3a). The expression level of *DDX1* in tumors with *MYCN* amplification alone was as low as that without *MYCN* amplification. Enhanced DDX1 expression had no significant correlation with prognosis ($p = 0.925$, log-rank test).

The expression level of *NAG* in *NAG* co-amplified tumors was significantly higher than that in tumors without *NAG* co-amplification ($p = 5.77 \times 10^{-6}$, Mann–Whitney's *U*-test); however, *NAG* amplification was not necessarily accompanied with enhanced *NAG* expression (Fig. 3b). Enhanced *NAG* expression had no significant relation to disease stage (stage 1, 2, 3, and 4s versus stage 4) ($p = 0.462$, Fisher's exact probability test) or clinical outcome ($p = 0.0915$, log-rank test).

Relation of *DDX1* and *NAG* gene expression statuses to survival probability for patients with *MYCN*-amplified NB

None of the gene expression statuses had a significant correlation with disease stage and with survival for patients aged <18 months (data not shown).

In 41 patients with *MYCN*-amplified NB aged ≥18 months, those with tumor with enhanced *DDX1* expression and low-*NAG* expression had a significantly better outcome than those with low-*DDX1* expression or enhanced *NAG* expression ($p = 0.0245$, log-rank test) (Fig. 4a, b). The 16 tumors with enhanced *DDX1* and low-*NAG* expression included one with stage 2, four with stage 3, and 11 tumors with stage 4. All 16 tumors had *MYCN* and *DDX1* co-amplification without *NAG* amplification.

Discussion

Amplification of the *MYCN* gene is strongly associated with the rapid progression of NB and advanced disease stage (Brodeur et al. 1984; Seeger et al. 1985). The prognosis of patients with stage 4 tumors with *MYCN* amplification had been extremely poor. In 1999, Kaneko et al. reported treatment results with improved survival rate of patients with advanced NB aged 1 year or older treated with an intensive induction and consolidation chemotherapy regimens (Kaneko et al. 1999). With the use of a more intensive induction regimen followed by hematopoietic stem cell transplantation for *MYCN*-amplified stage 4 patients, survival curves for those with or without *MYCN* amplification appeared similar. In other words, the prognosis of patients with stage 4 NB without *MYCN* amplification remained poor (Kaneko et al. 2002). Their assessment of *MYCN* amplification status was based on the Southern blot technique. Measuring an accurate *MYCN* copy number in tumors is essential in

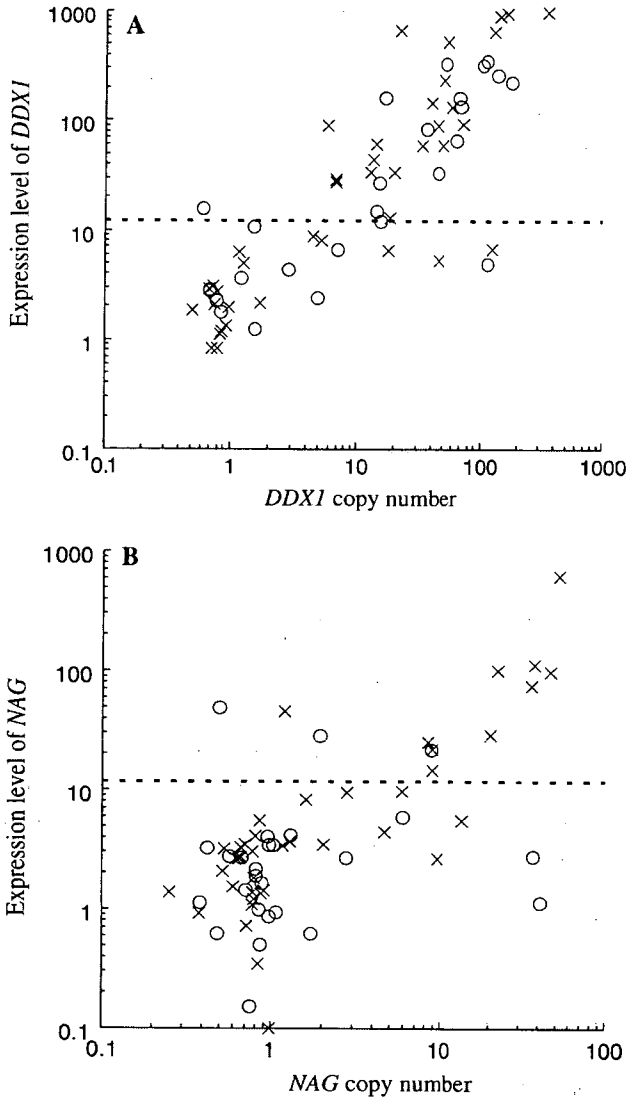

Fig. 3 Gene copy number and gene expression level of *DDX1* (**a**) and *NAG* (**b**) in 67 *MYCN*-amplified NBs. *Open circle*, survivors with *MYCN* amplification ($n = 26$); *cross*, nonsurvivors with *MYCN* amplification ($n = 41$); *dotted line*, the highest expression level of *DDX1* (**a**) or *NAG* (**b**) in *MYCN*-unamplified NBs

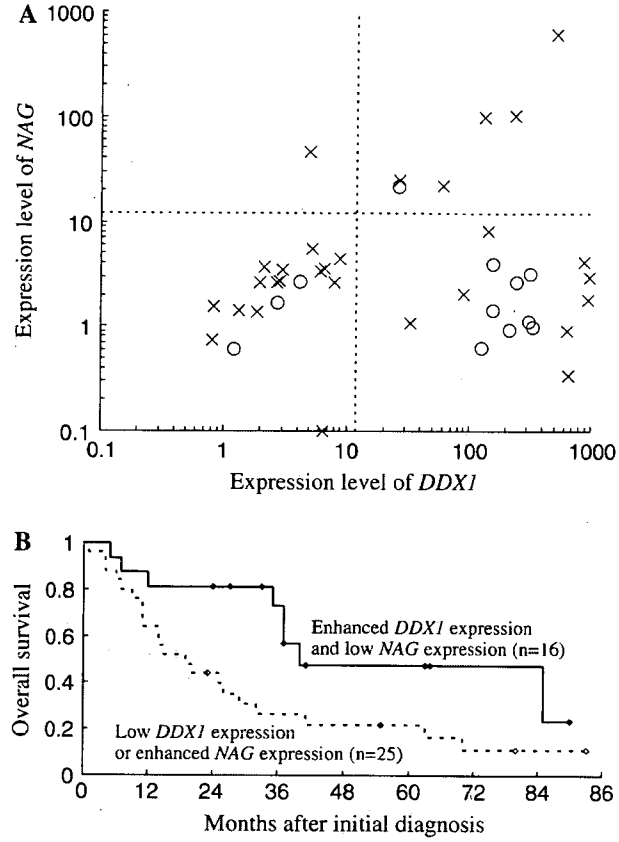

Fig. 4 **a** Expression level of *DDX1* and *NAG* mRNA in 41 *MYCN*-amplified NBs from patients aged ≥18 months. *Open circle*, survivors with *MYCN* amplification ($n = 12$); *cross*, nonsurvivors with *MYCN* amplification ($n = 29$); *dotted lines*, the highest expression levels of *DDX1* and *NAG* in *MYCN*-unamplified NBs. **b** In the 41 patients with *MYCN*-amplified NB aged ≥18 months, those with tumor with enhanced *DDX1* expression and low-*NAG* expression showed a significantly better outcome than those with low-*DDX1* expression or enhanced *NAG* expression ($p = 0.0245$, log-rank test)

order to select the optimal treatment and improve survival for patients with advanced NB. Assays for the rapid and accurate quantification of *MYCN* copy number and *MYCN* expression level in NB have been developed by real-time q-PCR or q-RT-PCR method with TaqMan probe (Raggi et al. 1999; Tajiri et al. 2001; De Preter et al. 2002). Tanaka et al. reported that in their highly sensitive analysis by a q-PCR method combined with FISH, cases with more than two *MYCN* gene dosages (*MYCN/p53* ≥2.0) were significantly associated with unfavorable prognostic factors (Tanaka et al. 2004). In our study, we did not investigate NBs with a haploid *MYCN* gene copy number of between two and five.

Recently, Scott et al. found that the 7.3 kb transcript of the *NAG* gene with 52 exons, which is predominantly expressed in NB, covers 420 kb of genomic DNA. They proposed that probes for Southern blot or FISH studies, or primers used for PCR-based methods, should include the 3′ end of the *NAG* gene over 400 kb away from *DDX1* (Scott et al. 2003b). The primers and TaqMan probe we designed were located on the 3′ end of the *NAG* gene, on exon 52, and the frequency of *NAG* co-amplification with *MYCN* was in accordance with that reported by Scott et al.

It is thought that a low copy number of *MYCN* in *MYCN*-amplified human NB cells is correlated with a low degree of recombination and large amplicon size (Amler and Schwab 1989). Consistent with the findings by Amler and Schwab, we found for the first time that NB with lower copies of *MYCN* amplification tended

to a more frequent *DDX1* and *NAG* co-amplification than those with higher copies of *MYCN*. For evaluating the frequency of *DDX1* and *NAG* co-amplification, it proved appropriate to discriminate NBs with <40 copies of *MYCN* amplification from those with ≥40 copies of *MYCN*. The information obtained from these observations may be different from a recent suggestion by De Preter et al. that the process of co-amplification within the *MYCN* amplicon occurs coincidentally, and is not subject to selection (De Preter et al. 2005).

The prognostic significance of DDX1 co-amplification with MYCN has remained unclear. Squire et al. analyzed 13 *MYCN*-amplified patients and showed a trend toward a worse clinical outcome with *DDX1* co-amplification (Squire et al. 1995). George et al. reported that with the exclusion of patients with 4S disease, those with *DDX1* co-amplification had a significantly shorter mean disease-free interval compared with *MYCN* amplification alone (George et al. 1997). However, they described that there was no significant difference in the proportion of survivors in these two groups. In contrast, Weber et al. reported that *DDX1* co-amplification correlated with an improved patient survival in 98 *MYCN*-amplified NB (Weber et al. 2004). In our study of 72 patients with *MYCN*-amplified NB, there was no significant difference in survival probability between patients with *DDX1*-co-amplified NB and those with tumor with *MYCN* amplification alone. The result was similar to those reported by Manohar et al. and De Preter et al. (Manohar et al. 1995; De Preter et al. 2002, 2005).

The *NAG* tended toward a more frequent co-amplification with *MYCN* in stage 4 compared with other stages, in contrast to the result of a significant association of *NAG* co-amplification with low-stage disease by Scott et al. (2003b). The difference was probably caused by the lower frequency of *NAG* co-amplification with *MYCN*. Amplification of *NAG* was not necessarily accompanied with enhanced *NAG* expression, and *NAG* expression level in *MYCN*-amplified tumors showed no significant relation to disease stage. The relationship between RNA expression levels of *DDX1* or *NAG* and clinical outcome for patients with *MYCN*-amplified NB has hardly been studied. Weber et al. reported that a high expression level of *DDX1* was associated with a trend toward a better survival probability while *NAG* expression was not correlated with prognosis (Weber et al. 2004). They drew the result using RNAs from 19 *MYCN*-amplified NB samples. We analyzed *DDX1* and *NAG* gene expression in 67 *MYCN*-amplified NB. Enhanced *DDX1* and *NAG* expression had no significant correlation with prognosis, respectively.

For the discrimination of prognosis for patients with NB, an age cut-off of 12 months was adopted worldwide. However, the International Neuroblastoma Pathology Classification, established for the prognostic evaluation of patients with neuroblastic tumors, has incorporated age factor of 18 months in the system (Shimada et al. 2001; Sano et al. 2006). The Children's Cancer Group in the USA has already chosen the 18 months as an age cut-off (Schmidt et al. 2005). Recent evidence supports the age cut-off ranging 15–18 months based on the results from the German analysis and two Children's Oncology Group analyses (London et al. 2005). In our study, the *DDX1* and *NAG* gene expression status in *MYCN*-amplified NBs revealed an age cut-off of 18 months to be an appropriate prognostic predictor of survival. We found that older patients with enhanced *DDX1* expression and low-*NAG* expression had a significantly better prognosis than those with low-*DDX1* expression or enhanced *NAG* expression. These findings indicate that, for *MYCN*-amplified NB from patients aged ≥18 months, both enhanced *DDX1* expression and low-*NAG* expression may be associated with a better response to intensive therapy. It is also possible to suggest a subset of NB in which enhanced *DDX1* and low-*NAG* expression consequent to *MYCN* and *DDX1* co-amplification without *NAG* amplification contributes to patient survival.

A larger cohort of patients and longer follow-up period using an age cut-off of 18 months will be required to clarify the clinical and prognostic significance of the expression status of both *DDX1* and *NAG* genes with *MYCN*.

References

Amler LC, Schwab M (1989) Amplified N-myc in human neuroblastoma cells is often arranged as clustered tandem repeats of differently recombined DNA. Mol Cell Biol 9:4903–4913

Beheshti B, Braude I, Marrano P, Thorner P, Zielenska M, Squire JA (2003) Chromosomal localization of DNA amplifications in neuroblastoma tumors using cDNA microarray comparative genomic hybridization. Neoplasia 5:53–62

Bleoo S, Sun X, Hendzel MJ, Rowe JM, Packer M, Godbout R (2001) Association of human DEAD box protein DDX1 with a cleavage stimulation factor involved in 3'-end processing of pre-MRNA. Mol Biol Cell 12:3046–3059

Brodeur GM, Seeger RC, Schwab M, Varmus HE, Bishop JM (1984) Amplification of N-myc in untreated human neuroblastoma correlates with advanced disease stage. Science 224:1121–1124

Brodeur GM, Seeger RC (1986) Gene amplification in human neuroblastoma: basic mechanisms and clinical implications. Cancer Genet Cytogenet 19:101–111

Chen HC, Lin WC, Tsay YG, Lee SC, Chang CJ (2002) An RNA helicase, DDX1, interacting with poly(A) RNA and hetero-

geneous nuclear ribonucleoprotein K. J Biol Chem 277: 40403–40409
Chomczynski P, Sacchi N (1987) Single-step method of RNA isolation by acid guanidium thiocyanate-phenol-chloroform extraction. Anal Biochem 162:156–159
De Preter K, Spelemam F, Combaret V, Lunec J, Laureys G, Eussen BH, Francotte N, Board J, Pearson AD, De Paepe A, Van Roy N, Vandesompele J (2002) Quantification of MYCN, DDX1, and NAG gene copy number in neuroblastoma using a real-time quantitative PCR assay. Mod Pathol 15:159–166
De Preter K, Spelemam F, Combaret V, Lunec J, Board J, Pearson A, De Paepe A, Van Roy N, Laureys G, Vandesompele J (2005) No evidence for correlation of DDX1 gene amplification with improved survival probability in patients with MYCN-amplified neuroblastomas. J Clin Oncol 23:3167–3168
De Valoir T, Tucker MA, Belikoff EJ, Camp LA, Bolduc C, Beckingham K (1991) A second maternally expressed Drosophila gene encodes a putative RNA helicase of the DEAD box family. Proc Natl Acad Sci USA 88:2113–2117
George RE, Kenyon R, McGuckin AG, Kohl N, Kogner P, Christiansen H, Pearson AD, Lunec J (1997) Analysis of candidate gene co-amplification with MYCN in neuroblastoma. Eur J Cancer 33:2037–2042
Godbout R, Squire JA (1993) Amplification of a DDX1 box protein gene in retinoblastoma cell lines. Proc Natl Acad Sci USA 90:7578–7582
Godbout R, Packer M, Katyal S, Bleoo S (2002) Cloning and expression analysis of the chicken DEAD box gene DDX1. Biochim Biophys Acta 1574:63–71
Iost I, Dreyfus M (1994) mRNAs can be stabilized by DEAD-box proteins. Nature 372:193–196
Kaneko M, Tsuchida T, Uchino J, Takeda T, Iwafuchi M, Ohnuma N, Mugishima H, Yokoyama J, Nishihira H, Nakada K, Sasaki S, Sawada T, Kawa K, Nagahara N, Suita S, Sawaguchi S (1999) Treatment results of advanced neuroblastoma with the first Japanese Study Group Protocol. J Pediatr Hematol Oncol 21:190–197
Kaneko M, Tsuchida T, Mugishima H, Ohnuma N, Yamamoto K, Kawa K, Iwafuchi M, Sawada T, Suita S (2002) Intensified chemotherapy increases the survival rates in patients with stage 4 neuroblastoma with MYCN amplification. J Pediatr Hematol Oncol 24:613–621
Kitajima Y, Yatsuki H, Zhang R, Matsuhashi S, Hori K (1994) A novel human homolog of a DEAD-box RNA helicase family. Biochem Biophys Res Commun 199:748–754
Kuroda H, White PS, Sulman EP, Manohar CF, Reiter JL, Cohn SL, Brodeur GM (1996) Physical mapping of the DDX1 gene to 340 kb 5' of MYCN. Oncogene 13:1561–1565
London WB, Boni L, Simon T, Berthold F, Twist C, Schmidt ML, Castleberry RP, Matthay KK, Cohn SL, De Bernardi B (2005) The role of age in neuroblastoma risk stratification: the German, Italian, and children's oncology group perspectives. Cancer Lett 228:257–266
Manohar CF, Salwen HR, Brodeur GM, Cohn SL (1995) Co-amplification and concomitant high levels of expression of a DEAD box gene with MYCN in human neuroblastoma. Genes Chromosomes Cancer 14:196–203
Raggi CC, Bagnoni ML, Tonini GP, Maggi M, Vona G, Pinzani P, Mazzocco K, De Bernardi B, Pazzagli M, Orlando C (1999) Real-time quantitative PCR for the measurement of MYCN amplification in human neuroblastoma with the TaqMan detection system. Clin Chem 45:1918–1924
Sano H, Bonadio J, Gerbing RB, London WB, Matthay KK, Lukens JN, Shimada H (2006) International neuroblastoma pathology classification adds independent prognostic information beyond the prognostic contribution of age. Eur J Cancer 42:1113–1119
Schmid SR, Linder P (1992) D-E-A-D protein family of putative RNA helicases. Mol Microbiol 6:283–291
Schmidt ML, Lal A, Seeger RC, Maris JM, Shimada H, O'Leary M, Gerbing RB, Matthay KK (2005) Favorable prognosis for patients 12 to 18 months of age with stage 4 nonamplified MYCN neuroblastoma: a Children's Cancer Group Study. J Clin Oncol 23:6474–6480
Scott D, Elsden J, Pearson A, Lunec J (2003a) Genes co-amplified with MYCN in neuroblastoma: silent passengers or co-determinants of phenotype? Cancer Lett 197:81–86
Scott DK, Board JR, Lu X, Pearson AD, Kenyon RM, Lunec J (2003b) The neuroblastoma amplified gene, NAG: genomic structure and characterisation of the 7.3 kb transcript predominantly expressed in neuroblastoma. Gene 307:1–11
Seeger RC, Brodeur GM, Sather H, Dalton A, Siegel SE, Wong KY, Hammond D (1985) Association of multiple copies of the N-myc oncogene with rapid progression of neuroblastomas. N Engl J Med 313:1111–1116
Shimada H, Umchara S, Monobe Y, Hachitanda Y, Nakagawa A, Goto S, Gerbing RB, Stram DO, Lukens JN, Matthay KK (2001) International neuroblastoma pathology classification for prognostic evaluation of patients with peripheral neuroblastic tumors: a report from the Children's Cancer Group. Cancer 92:2451–2461
Squire JA, Thorner PS, Weitzman S, Maggi JD, Dirks P, Doyle J, Hale M, Godbout R (1995) Co-amplification of MYCN and a DEAD box gene (DDX1) in primary neuroblastoma. Oncogene 10:1417–1422
Tajiri T, Tanaka S, Shono K, Kinoshita Y, Fujii Y, Suita S, Ihara K, Hara T (2001) Quick quantitative analysis of gene dosages associated with prognosis in neuroblastoma. Cancer Lett 166:89–94
Tanaka S, Tajiri T, Noguchi S, Shono K, Ihara K, Hara T, Suita S (2004) Clinical significance of a highly sensitive analysis for gene dosage and the expression level of MYCN in neuroblastoma. J Pediatr Surg 39:63–68
Tanner NK, Linder P (2001) DExD/H box RNA helicases: from generic motors to specific dissociation functions. Mol Cell 8:251–262
Vandesompele J, Speleman F, Van Roy N, Laureys G, Brinkschmidt C, Christiansen H, Lampert F, Lastowska M, Bown N, Pearson A, Nicholson JC, Ross F, Combaret V, Delattre O, Feuerstein BG, Plantaz D (2001) Multicentre analysis of patterns of DNA gains and losses in 204 neuroblastoma tumors: How many genetic subgroups are there? Med Pediatr Oncol 36:5–10
Weber A, Imisch P, Bergmann E, Christiansen H (2004) Coamplification of DDX1 correlates with an improved survival probability in children with MYCN-amplified human neuroblastoma. J Clin Oncol 22: 2681–2690

Oxidative stress induces p53-dependent apoptosis in hepatoblastoma cell through its nuclear translocation

Hideki Yamamoto[1,2], Toshinori Ozaki[1], Mitsuru Nakanishi[1], Hironobu Kikuchi[1], Kaori Yoshida[1], Hiroshi Horie[3], Hiroyuki Kuwano[2] and Akira Nakagawara[1,*]

[1]*Division of Biochemistry, Chiba Cancer Center Research Institute, Chiba 260-8717, Japan*
[2]*Department of General Surgical Science (Surgery 1), Gunma University, Graduate School of Medicine, Maebashi 371-8511, Japan*
[3]*Chiba Children's Hospital, Chiba 266-0007, Japan*

Hepatoblastoma (HBL) is the most common malignant liver tumor in children. Since tumor suppressor p53 is rarely mutated in HBL, it remains unknown whether p53 could contribute to the hepatocarcinogenesis. In the present study, we have found for the first time that, like neuroblastoma (NBL), wild-type p53 was abnormally accumulated in the cytoplasm of the human HBL-derived Huh6 cells. In accordance with this notion, immunohistochemical analysis demonstrated that p53 is largely expressed in cytoplasm of human primary HBLs. In response to the oxidative stress, Huh6 cells underwent apoptotic cell death in association with the nuclear translocation of p53 and the transactivation of its target gene implicated in apoptotic cell death. siRNA-mediated knockdown of the endogenous p53 conferred the resistance of Huh6 cells to oxidative stress. Intriguingly, histone deacetylase inhibitor (nicotinamide) treatment strongly inhibited the oxidative stress-induced nuclear translocation of p53 as well as the p53-dependent apoptosis in Huh6 cells. In contrast to the previous observations, the cytoplasmic anchor protein for p53 termed Parc had undetectable effect on the cytoplasmic retention of p53. Collectively, our present results suggest that the abnormal cytoplasmic localization of p53 might contribute at least in part to the development of HBL.

Introduction

Hepatoblastoma (HBL) is one of the most frequent malignant liver tumors of childhood. Indeed, its incidence is higher than that of hepatocellular carcinoma (HCC) in children. HBL arises from the hepatic precursor cells and displays a morphological similarity to the immature hepatocytes of the developing liver. In a sharp contrast to HCC, which is associated with hepatitis virus infection (Llovet *et al.* 2003), it has been shown that the incidence of HBL is highly elevated in patients with familial adenomatous polyposis (FAP), which carry germ-line mutations in the APC (adenomatous polyposis coli) tumor suppressor gene (Hughes & Michels 1992; Nagase & Nakamura 1993). APC protein forms a cytoplasmic multiprotein complex involved in the Wnt signaling pathway, which regulates the stability of β-catenin (Henderson & Fagotto 2002). Although APC is rarely mutated in sporadic HBL, accumulating evidence demonstrated that the frequent mutations or deletions of β-catenin at hot-spot regions within the exon 3 encoding its degradation targeting box are detectable in HBL, suggesting that the abnormal nuclear accumulation of the stabilized β-catenin which collaborates with Tcf/Lef complex plays a central role in the genesis of HBL (Koch *et al.* 1999). Consistent with this notion, Takayasu *et al.* (2001) revealed that β-catenin mutation is significantly correlated with the up-regulation of its target genes, including cyclin D1 and fibronectin. However, Harada *et al.* (2002, 2004) described that β-catenin mutation alone is not sufficient for the hepatocarcinogenesis, indicating that the additional mutations or epigenetic changes might be required for the genesis of HBL. The detailed molecular mechanism(s) behind the pathogenesis and development of HBL remains unknown.

The p53 tumor suppressor is a nuclear transcription factor, which has an ability to transactivate various p53-target genes implicated in the regulation of G1 cell cycle arrest and/or apoptosis such as $p21^{WAF1}$, MDM2, Bax and NOXA (Prives & Hall 1999; Sionov & Haupt 1999; Vousden & Lu 2002). The importance of p53 in the tumorigenesis has been emphasized by the observations

Communicated by: Takeo Kishimoto
**Correspondence*: E-mail: akiranak@chiba-cc.jp

DOI: 10.1111/j.1365-2443.2007.01065.x

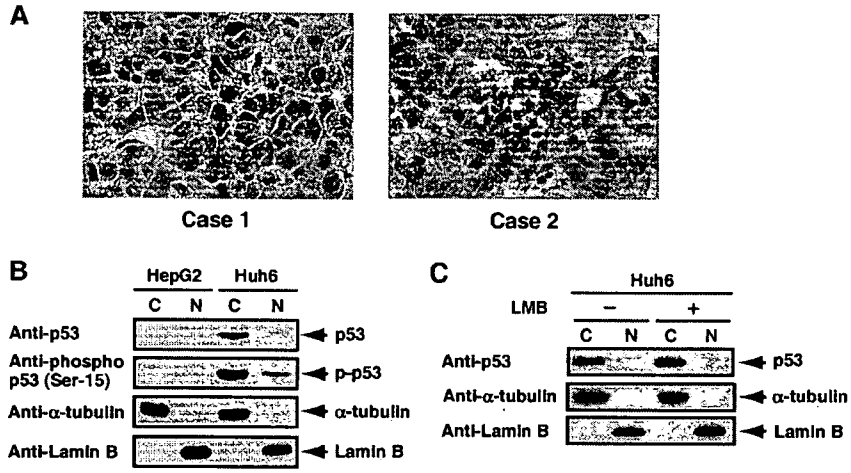

Figure 1 Cytoplasmic localization of p53 in HBL cells. (A) Immunohistochemical analysis. Sections (4 μm thick) of two primary hepatoblastoma tissues (case 1 and 2) were stained with the anti-p53 antibody. Note the positive signals in the cytoplasm of most tumor cells. (B) p53 is abundantly expressed in cytoplasm of Huh6 cells. Huh6 and HepG2 cells were biochemically fractionated into cytoplasmic (C) and nuclear (N) fractions as described under Experimental procedures. Equal amounts of cytoplasmic and nuclear extracts were subjected to Western blotting with the anti-p53 or with the anti-phosphorylated form of p53 at Ser-15. α-tubulin and Lamin B were used for the cytoplasmic and nuclear markers, respectively. (C) Leptomycin B has undetectable effect on the subcellular localization of p53. Huh6 cells were treated with or without 20 ng/mL of Leptomycin B (LMB). Six hours after the treatment, cells were fractionated into cytoplasmic (C) and nuclear (N) fractions, and subjected to Western blotting with the indicated antibodies.

showing that p53 mutation is detected in more than half of all human tumors (Hollstein *et al.* 1991; Vogelstein *et al.* 2000). The tumor-suppressive activity of p53 is dependent on its sequence-specific transactivation function. Indeed, the vast majority of p53 mutations are found within its central sequence-specific DNA-binding domain. Under normal conditions, p53 is a short-lived protein whose expression levels are kept extremely low. MDM2 acts as an E3 ubiquitin protein ligase for p53, and promotes its ubiquitination followed by degradation by 26S proteasome (Haupt *et al.* 1997; Honda *et al.* 1997; Kubbutat *et al.* 1997). Recently, it has been demonstrated that, like MDM2, Pirh2 and COP1 target p53 for degradation by 26S proteasome in an ubiquitin-dependent manner (Leng *et al.* 2003; Dornan *et al.* 2004). In response to genotoxic stresses, p53 is induced to be accumulated in cell nucleus through its phosphorylation at multiple sites, including Ser-15, Ser-20 and Ser-46, and exerts its pro-apoptotic activity (Sionov & Haupt 1999; Vousden & Lu 2002). In addition to the NH_2-terminal phosphorylation of p53, p300/CBP (CREB-binding protein) with the histone acetyltransferase (HAT) activity binds to the NH_2-terminal region of p53, mediates the acetylation of its COOH-terminal region and thereby enhances its activity (Gu & Roeder 1997). Thus, the post-translational modifications of p53 enhance its transcriptional as well as pro-apoptotic ability.

In contrast to other human tumors, p53 is infrequently mutated in certain human tumors such as neuroblastoma (NBL) and HBL (Vogan *et al.* 1993; Chen *et al.* 1995; Ohnishi *et al.* 1996; Kusafuka *et al.* 1997), indicating that p53 plays no role in the genesis and development of these tumors. However, this viewpoint has been challenged by the observations that the wild-type p53 is abnormally accumulated in the cytoplasm of NBLs (Moll *et al.* 1995). These findings strongly suggest that the nuclear exclusion of wild-type p53 might represent one non-mutational mechanism of p53 inactivation. In addition to NBL, wild-type p53 is abnormally sequestered in the cytoplasm in certain human tumors, including breast and colon cancers (Moll *et al.* 1992; Bosari *et al.* 1995). Although the detailed molecular mechanism(s) of the cytoplasmic accumulation of wild-type p53 remains unclear, Nikolaev *et al.* (2003) described that Parc (p53-associated parkin-like cytoplasmic protein) interacts with p53 in cytoplasm and inhibits its nuclear translocation.

In the present study, we have found that wild-type p53 is abundantly expressed in human primary HBLs and HBL-derived Huh6 cells. In response to oxidative stress, p53 was induced to be translocated into cell nucleus of Huh6 cells, and Huh6 cells underwent apoptotic cell death. Furthermore, nicotinamide treatment abolished the oxidative stress-induced nuclear translocation of p53, thereby inhibiting the p53-dependent apoptotic cell death.

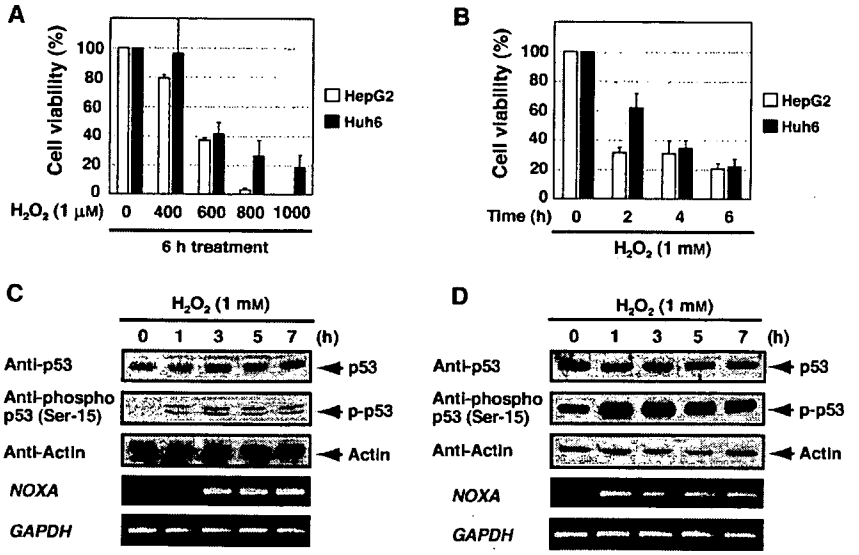

Figure 2 Effect of H_2O_2 treatment on Huh6 and HepG2 cell lines. (A, B) MTT cell survival assays. Huh6 (filled boxes) and HepG2 cells (open boxes) were exposed to H_2O_2 at the indicated concentrations for 6 h. After the treatment with H_2O_2, their cell viability was assessed by MTT assays (A). Similarly, Huh6 and HepG2 cells were treated with 1 mM of H_2O_2 for the indicated time periods, and their cell viability was examined by MTT assays (B). (C, D) Western blot analysis. HepG2 (C) and Huh6 cells (D) were treated with 1 mM of H_2O_2 for the indicated periods of time. Thereafter, whole cell lysates were prepared, and subjected to Western blotting with the anti-p53 (1st panel) or with anti-phospho-p53 at Ser-15 (2nd panel). Expression of actin was used to control equal protein loading (3rd panel). Alternatively, total RNA was extracted from cells treated with H_2O_2, and analyzed by RT-PCR for the expression of NOXA (4th panel). GAPDH was used to normalize (5th panel).

Results

Cytoplasmic expression of p53 in human HBLs

As previously described (Vogan *et al.* 1993; Moll *et al.* 1995), p53 is rarely mutated in human primary NBLs, and predominantly expressed in cytoplasm. Similar to NBLs, it has been shown that p53 is infrequently mutated in human primary HBLs (Chen *et al.* 1995; Ohnishi *et al.* 1996); however, its subcellular localization remains unclear. Then, we sought to examine the subcellular localization of p53 in surgically resected specimens of primary HBLs by immunohistochemistry. As shown in Fig. 1A, p53 immunoreactivity was detectable largely in cytoplasm of tumor cells, suggesting that, like NBLs, p53 might lack its intact function due to its abnormal cytoplasmic localization in HBLs. To further confirm these observations, we examined the subcellular distribution of p53 in HBL-derived Huh6 (Doi 1976) and HCC-derived HepG2 cells (Aden *et al.* 1979). As described (Bressac *et al.* 1990; Hsu *et al.* 1993), HepG2 cells carry wild-type p53. Our sequence analysis revealed that p53 expressed in Huh6 cells has a wild-type structure (data not shown). Huh6 and HepG2 cells were biochemically fractionated into cytoplasmic and nuclear fractions, and subjected to Western blotting with the anti-p53 antibody. α-tubulin and Lamin B were used as cytoplasmic and nuclear markers, respectively. Under our experimental conditions, E-cadherin, which is one of the membrane marker, was detected in the cytoplasmic fraction (data not shown). As shown in Fig. 1B, p53 was undetectable in each fraction of HepG2 cells, whereas p53 was largely expressed in cytoplasm of Huh6 cells, which was consistent with our immunohistochemical analysis of primary HBLs. It is worth noting that p53 is constitutively phosphorylated at Ser-15 in Huh6 cells in the absence of DNA damage. To rule out a possibility that the subcellular localization of p53 could be regulated by active nuclear export in Huh6 cells, Huh6 cells were treated with the nuclear export inhibitor leptomycin B (LMB). As shown in Fig. 1C, LMB had undetectable effect on the subcellular distribution of p53 in Huh6 cells.

Induction of apoptosis by oxidative stress in HBL-derived and HCC-derived cell lines

As described (Lluis *et al.* 2005), oxidative stress induced apoptotic cell death in hepatocytes. To examine a possible effect of the oxidative stress on Huh6 and HepG2 cells, these cells were treated with H_2O_2, and their cell viability was assessed by MTT cell survival assay. As shown in Fig. 2 A,B, Huh6 and HepG2 cells underwent apoptosis

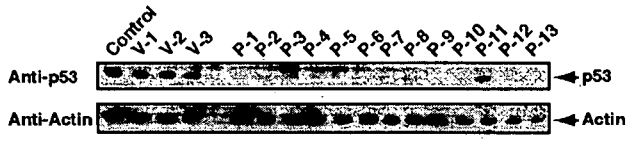

Figure 3 siRNA-mediated knockdown of p53 in Huh6 cells. Huh6 cells were stably transfected with the empty plasmid (V1–V3) or with the expression plasmid encoding siRNA against p53 (P1–P13), and cultured in the presence of G418 (at a final concentration of 400 μg/mL) for 2 weeks. Whole cell lysates prepared from the indicated cell clones and the parental Huh6 cells (Control) were analyzed by Western blotting for the expression levels of the endogenous p53 and actin.

in response to H_2O_2 in a dose-dependent and a time-dependent manner. Since p53 plays a central role in the DNA damage-induced apoptosis (Prives & Hall 1999; Sionov & Haupt 1999), we examined the changes in endogenous p53 protein levels following treatment with H_2O_2. As shown in Fig. 2C, p53 was expressed at low levels in HepG2 cells without H_2O_2. Following exposure to H_2O_2, p53 was induced to be accumulated in association with a remarkable increase in the amounts of p53 phosphorylated at Ser-15. RT-PCR analysis revealed that the transcription levels of pro-apoptotic NOXA, which is one of the p53-target genes, are elevated in response to H_2O_2 treatment. In contrast, the amounts of total p53 remained almost constant and p53 was constitutively phosphorylated at Ser-15 in Huh6 cells regardless of H_2O_2 treatment (Fig. 2D). Under our experimental conditions, however, the expression levels of NOXA were increased in Huh6 cells exposed to H_2O_2, suggesting that p53 might contribute to the oxidative stress-mediated apoptotic cell death in Huh6 cells.

p53 plays a critical role in the H_2O_2-mediated apoptosis in Huh6 cells

To examine whether p53 could play an important role in the regulation of H_2O_2-dependent apoptosis in Huh6 cells, Huh6 cells were stably transfected with the expression plasmid encoding siRNA against p53 or with its control plasmid. Two weeks after the selection with G418 (at a final concentration of 400 μg/mL), we finally established several p53-knockdown cell clones as well as control cell clones (Fig. 3). We then investigated their sensitivity to H_2O_2 by TUNEL staining. Five hours after the treatment with H_2O_2 at a final concentration of 1 mM, V-2, V-3, P-9 and P-10 cells were subjected to TUNEL staining to identify the apoptotic cells. Cell nuclei were stained with DAPI. As shown in Fig. 4, exposure of V-2 and V-3 cells to H_2O_2 resulted in a significant increase in a number of TUNEL-positive cells, whereas two to threefold decrease in a number of cells with apoptotic nuclei was observed in P-9 and P-10 cells in response to H_2O_2. Similar results were also obtained in the other cell clones (data not shown). These results strongly suggest that p53 contributes at least in part to the H_2O_2-mediated apoptotic cell death in Huh6 cells.

H_2O_2-mediated nuclear translocation of p53

It is well documented that p53 is induced to be accumulated in cell nucleus in response to various DNA damaging agents, including cisplatin (CDDP) (Fritsche *et al.* 1993). In accordance with this notion, CDDP treatment stimulated the nuclear accumulation of p53 in Huh6 cells in a time-dependent manner, whereas the amounts of cytoplasmic p53 remained unchanged regardless of CDDP treatment (Fig. 5A). Additionally, Huh6 cells underwent apoptotic cell death in response to CDDP (Fig. 5B). Intriguingly, there existed an inverse relationship between the amounts of cytoplasmic and nuclear p53 in response to H_2O_2 (Fig. 5C). Indirect immunofluorescent staining indicated that p53 is largely expressed in cytoplasm of Huh6 cells, whereas p53 accumulates in cell nucleus in response to H_2O_2 (Fig. 5D). Thus, it is likely that the H_2O_2-mediated nuclear translocation of p53 might be one of the molecular mechanisms underlying the H_2O_2-dependent apoptosis in Huh6 cells.

Parc has an undetectable effect on the cytoplasmic retention of p53

The nuclear localization of p53 is critical for its transcriptional activity as well as apoptosis-inducing function. Recently, Nikolaev *et al.* (2003) have found that a Parkin-like ubiquitin ligase termed Parc acts as cytoplasmic anchor protein to block nuclear localization of p53. To ask whether Parc could be involved in the cytoplasmic retention of p53 in Huh6 cells, we examined the interaction between p53 and Parc by immunoprecipitation experiments. Whole cell lysates prepared from Huh6 cells were immunoprecipitated with normal mouse serum (NMS) or with the anti-p53 antibody, and the immunoprecipitates were analyzed by Western blotting with the anti-Parc antibody. Consistent with the previous results (Nikolaev *et al.* 2003), the anti-p53 immunoprecipitates contained the endogenous Parc (Fig. 6A). We then examined a possible effect of Parc on the subcellular distribution of p53. For this purpose, Huh6 cells were transiently transfected with siRNA against Parc or with the control siRNA. Twenty-four hours after transfection, total RNA and

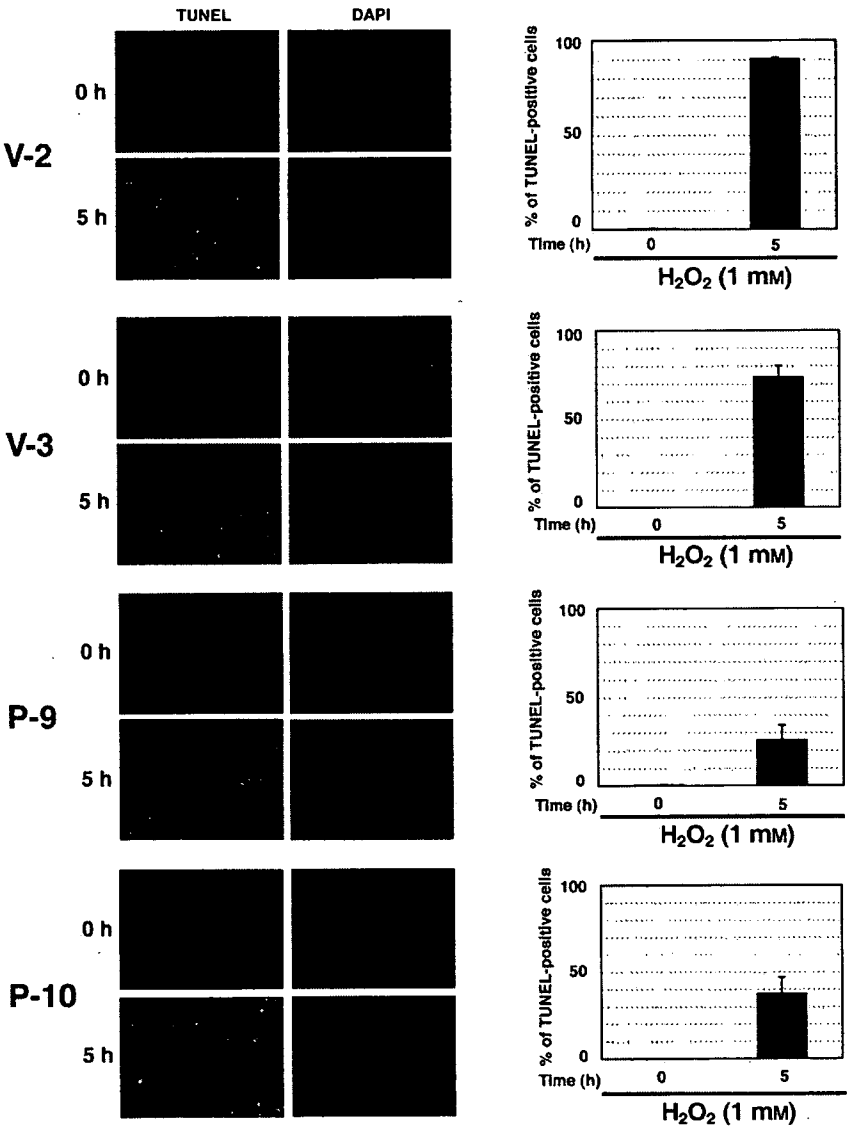

Figure 4 p53 is required for the H_2O_2-induced apoptosis in Huh6 cells. TUNEL staining. The indicated cell clones were treated with H_2O_2 at a final concentration of 1 mM or left untreated. Five hours after the treatment with H_2O_2, apoptotic cells were identified by TUNEL assay as described under Experimental procedures. The cell nuclei were stained with DAPI (left panels). The number of TUNEL-positive cells was counted, and expressed as a percentage of the total number of cells examined (right panels). H_2O_2-induced apoptosis was significantly different in cells expressing siRNA against p53 as compared with control cells. $P < 0.05$.

cytoplasmic/nuclear fractions were prepared and subjected to RT-PCR and Western blotting with the anti-Parc antibody, respectively. As shown in Fig. 6B, siRNA against Parc successfully reduced the expression levels of the endogenous Parc. Unexpectedly, siRNA-mediated knock-down of the endogenous Parc had a negligible effect on the subcellular localization of p53 in Huh6 cells as examined by Western blotting (Fig. 6C).

Nicotinamide treatment inhibits the H_2O_2-mediated nuclear translocation of p53 and apoptosis

Recently, it has been shown that the chemical modifications including acetylation regulate the subcellular localization of p53 (Kawaguchi *et al.* 2006). We then examined a possible effect of histone deacetylase inhibitor nicotinamide (Nico) on the H_2O_2-mediated nuclear translocation of p53 and p53-dependent apoptotic cell death. To this end, Huh6 cells were treated with the indicated combinations of drug. At the indicated time periods after the treatment, cells were biochemically fractionated into cytoplasmic and nuclear fractions, and subjected to Western blotting with the anti-p53 antibody. As shown in Fig. 7A, nicotinamide significantly inhibited the H_2O_2-mediated nuclear translocation of p53. Next, we sought to address whether nicotinamide could affect the H_2O_2-induced apoptosis. For this purpose, Huh6 cells were exposed to the indicated combinations of drug, and the number of TUNEL-positive cells was measured. As shown in Fig. 7B, nicotinamide treatment markedly inhibited

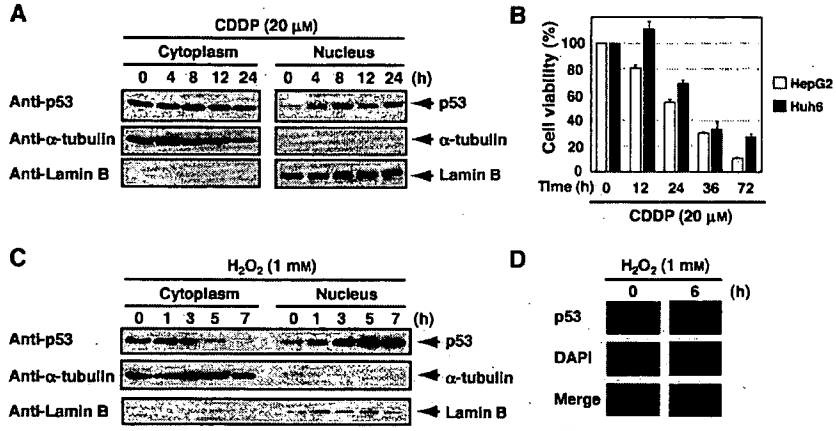

Figure 5 Nuclear translocation of p53 in response to H_2O_2. (A) CDDP-induced nuclear accumulation of p53. Huh6 cells were treated with 20 μM of CDDP. At the indicated time points after the treatment, cells were collected and fractionated into cytoplasmic and nuclear fractions, followed by Western blotting with the indicated antibodies. (B) CDDP-induced apoptotic cell death of Huh6 cells. At the indicated time periods after the exposure to CDDP (20 μM), Huh6 cells were subjected to MTT assay. (C) H_2O_2-mediated nuclear translocation of p53 in Huh6 cells. At the indicated time periods after the treatment with H_2O_2 (1 mM), Huh6 cells were fractionated into cytoplasmic and nuclear fractions, and subjected to Western blotting with the indicated antibodies. (D) Indirect immunofluorescence. Huh6 cells were treated with H_2O_2 (1 mM) or left untreated, and stained with anti-p53 antibody (red). Cells were costained with DAPI (blue) to reveal cell nucleus.

the H_2O_2-induced apoptotic cell death as compared with H_2O_2 alone. Similar results were also obtained in MTT assays (Fig. 7C). Together, our results strongly suggest that the acetylation status might be critical for the H_2O_2-induced nuclear translocation of p53 and apoptosis in HBL cells.

Discussion

p53 acts as a tumor suppressor by inducing cell cycle arrest and/or apoptotic cell death in tumor cells. It has been well documented that p53 mutation is found in over 50% of all human tumors, resulting in the loss of its pro-apoptotic function (Hollstein *et al.* 1991; Vogelstein *et al.* 2000). The pro-apoptotic function of p53 can be also abrogated by non-mutational mechanisms (Prives & Hall 1999). For example, p53 is infrequently mutated in human NBL; however, p53 is largely localized in cytoplasm, indicating that p53 has no role in the genesis and development of NBL (Vogan *et al.* 1993). Like NBL, extensive studies on the p53 status demonstrated the absence of mutations in HBL (Chen *et al.* 1995; Ohnishi *et al.* 1996). Although β-catenin is frequently mutated in HBL (Koch *et al.* 1999; Takayasu *et al.* 2001), recent studies suggest that β-catenin mutation alone is not sufficient for hepatocarcinogenesis (Harada *et al.* 2002; Harada *et al.* 2004). In the present study, we have found that p53 is exclusively expressed in cytoplasm of human primary HBL as well as HBL-derived Huh6 cells. In response to oxidative stress, p53 was translocated into cell nucleus, and exerted its pro-apoptotic function. Intriguingly, histone deacetylase inhibitor treatment strongly inhibited the oxidative stress-induced nuclear access of p53. Thus, it is likely that the cytoplasmic retention of p53, which might be mediated by acetylation, contributes at least in part to the genesis and development of HBL.

As mentioned above, the previous studies demonstrated that wild-type p53 is significantly accumulated in cytoplasm of human NBL (Moll *et al.* 1995; Ostermeyer *et al.* 1996). According to their results, the treatment of NBL-derived cells with p53 COOH-terminal peptide resulted in the relocalization of p53 to the cell nucleus, suggesting that the COOH-terminal region of p53 contributes to its cytoplasmic retention. As described (Stommel *et al.* 1999), p53 shuttles between cell nucleus and cytoplasm in its potential COOH-terminal nuclear export signal (NES) and its receptor Crm-1-dependent manner. Based on our present results, however, the nuclear export inhibitor LMB treatment had undetectable effect on the subcellular localization of p53 in Huh6 cells, suggesting that the NES-mediated efficient nuclear export is not involved in a significant cytoplasmic accumulation of p53 in Huh6 cells. Nikolaev *et al.* (2003) found that Parc prevents the nuclear translocation of p53 through the interaction with its lysine-rich COOH-terminal region which contains the nuclear localization signals (NLSs), and also suggested that their interaction might be regulated by post-translational modifications of p53 such as phosphorylation and/or

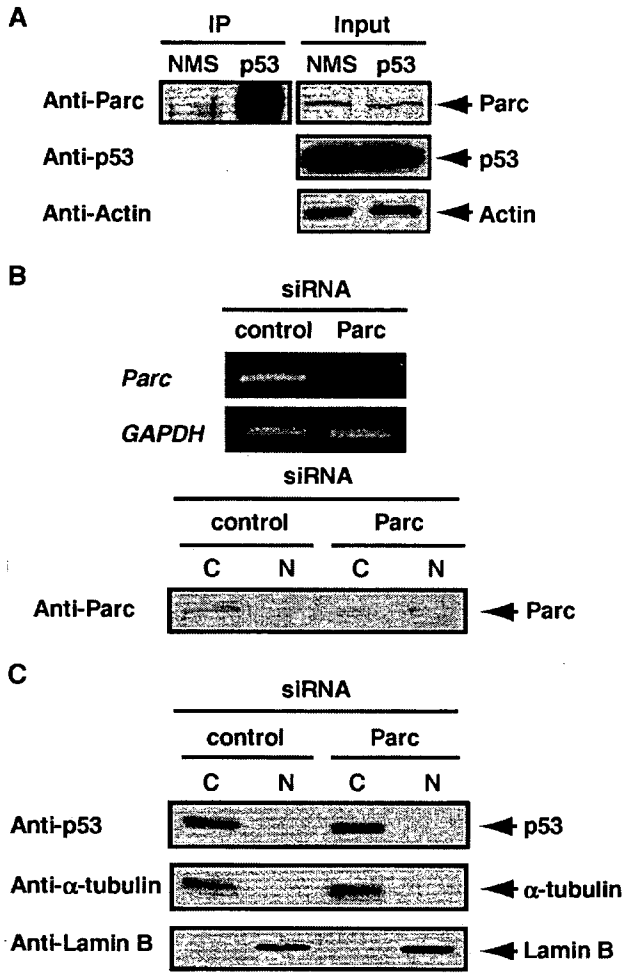

Figure 6 Parc has an undetectable effect on the subcellular localization of p53. (A) Parc is associated with p53 in Huh6 cells. Whole cell lysates prepared from Huh6 cells were immunoprecipitated with normal mouse serum (NMS) or with the anti-p53 antibody. The immunoprecipitates were analyzed by Western blotting with the anti-Parc antibody. Input corresponds to 5% of the whole cell lysates used in this assay. (B) siRNA-mediated knockdown of the endogenous Parc. Huh6 cells were transiently transfected with siRNA against Parc or with the control siRNA. Twenty-four hours after transfection, total RNA and cytoplasmic (C) nuclear (N) fractions were prepared and processed for RT-PCR and Western blotting with the anti-Parc antibody, respectively. (C) siRNA-mediated knockdown does not lead to the nuclear access of p53. Huh6 cells were transiently transfected with siRNA against Parc or with the control siRNA. Twenty-four hours after transfection, cells were fractionated into cytoplasmic (C) and nuclear fractions (N), and subjected to Western blotting with the indicated antibodies.

acetylation. Unexpectedly, our present results revealed that Parc binds to p53 in Huh6 cells; however, the cytoplasmic retention of p53 in Huh6 cells is regulated in a Parc-independent manner. It is worth noting that the nicotinamide treatment of Huh6 cells leads to the inhibition of the oxidative stress-induced nuclear access of p53 as well as the pro-apoptotic activity of p53, indicating that the acetylation status of p53 plays an important role in the regulation of the cytoplasmic retention of p53.

It is well documented that p300/CBP-mediated acetylation of p53 at the COOH-terminal lysine residues including Lys-320, Lys-370, Lys-371, Lys-372, Lys-381 and Lys-382 enhances the transcriptional activity as well as stability of p53 (Brooks & Gu 2003). p300/CBP possess histone acetyl-transferase (HAT) activity (Ogryzko *et al.* 1996). Since the COOH-terminal lysine residues of p53 are tightly associated with the p300/CBP-mediated acetylation as well as the MDM2-mediated ubiquitination, it is possible that p53 acetylation catalyzed by p300/CBP reduces its ubiquitination levels by competition between acetylation and ubiquitination. Alternatively, Kawaguchi *et al.* (2006) described that the hyperacetylated forms of p53 are accumulated in cytoplasm. Histone deacetylases are divided into three classes including class I, II and III (de Ruijter *et al.* 2003). Among them, class III histone deacetylases are distinct from the remaining classes, and defined based on their similarity to the yeast silent information regulator 2 (Sir2). One of the human Sir2 homologues, SIRT2, was largely localized in cytoplasm of mammalian cultured cells, and its catalytic activity was significantly inhibited by nicotinamide (North *et al.* 2003). In addition, SIRT1, another member of the class III histone deacetylases, was sensitive to nicotinamide, and had an ability to deacetylate p53 at Lys-382 (Michishita *et al.* 2005). Although it remains unclear whether SIRT2 could deacetylate p53, it is likely that SIRT family member(s) might be involved in the regulation of the oxidative stress-induced nuclear translocation of p53 in Huh6 cells. However, the precise molecular mechanisms behind the cytoplasmic localization of p53 in HBL are still unknown.

According to our present findings, p53 was constitutively phosphorylated at Ser-15 and stabilized in cytoplasm of Huh6 cells. Accumulating evidence suggests that MDM2 binds to the NH_2-treminal region of p53, acts as an E3 ubiquitin protein ligase for p53 and thereby promotes its proteasome-dependent proteolytic degradation (Chen *et al.* 1993; Haupt *et al.* 1997; Honda *et al.* 1997; Kubbutat *et al.* 1997). Previous studies demonstrated that the DNA damage-induced phosphorylation of p53 at Ser-15 mediated by ATM, ATR and/or DNA-PK disrupts the

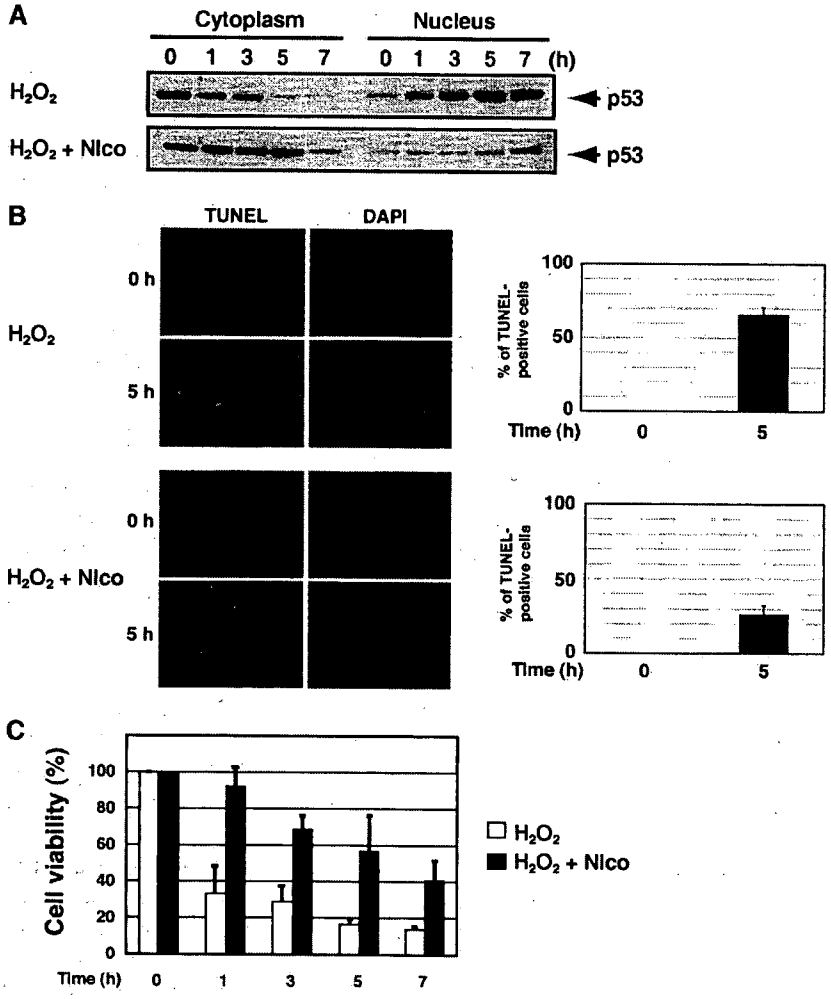

Figure 7 Deacetylase inhibitor nicotinamide inhibits the H_2O_2-mediated nuclear translocation of p53 and apoptotic cell death in Huh6 cells. (A) Huh6 cells were treated with H_2O_2 alone (1 mM) or with H_2O_2 (1 mM) plus nicotinamide (Nico, 5 mM). At the indicated time periods after the treatment with the drugs, cells were harvested and fractionated into cytoplasmic and nuclear fractions followed by Western blotting with the anti-p53 antibody. (B) TUNEL staining. Huh6 cells were exposed to the indicated combinations of the drug for 5 h. Apoptotic cells were identified by TUNEL assays. Cell nuclei were visualized by DAPI (left panels). The number of TUNEL-positive cells was scored, and expressed as a percentage of the total number of cells examined (right panels). H_2O_2-mediated apoptosis was significantly inhibited by nicotinamide. $P < 0.02$. (C) MTT cell survival assay. Huh6 cells were treated with the indicated combinations of the drug for 5 h or left untreated, and their viability was examined by MTT assays.

interaction between p53 and MDM2, resulting in the activation and stabilization of p53 (Shieh *et al.* 1997). Although the precise molecular mechanisms behind the constitutive phosphorylation of cytoplasmic p53 at Ser-15 remain unclear, it is likely that the significant accumulation of p53 in Huh6 cells without DNA damage might be due to the inhibition of the MDM2-mediated ubiquitination and proteasomal degradation of p53.

It has been shown that β-catenin, which is a key component of the Wnt signaling pathway, is frequently mutated or deleted in HBLs (Koch *et al.* 1999; Takayasu *et al.* 2001). These alterations occur in the NH_2-terminal region of β-catenin, which is responsible for the GSK3β-mediated phosphorylation (Aberle *et al.* 1997). Similar to the primary HBLs, HBL-derived Huh6 cells carry a mutant form of β-catenin at Thr-41 (Koch *et al.* 1999). GSK3β-mediated phosphorylation of β-catenin is required for its ubiquitin-dependent proteolytic degradation by 26S proteasome (Aberle *et al.* 1997). In accordance with this notion, a large amount of β-catenin was detectable in Huh6 cells in the absence of oxidative stress (data not shown). Intriguingly, it has been shown that DNA damage induces the nuclear accumulation of p53 as well as GSK3β, and p53 forms a stable complex with GSK3β (Watcharasit *et al.* 2002; Watcharasit *et al.* 2003). According to their results, p53 enhances the activity of GSK3β through the direct interaction with GSK3β in a phosphorylation-independent manner, and GSK3β activates the p53-dependent apoptotic pathway in response to DNA damage. Of note, we found that GSK3β was induced to be accumulated in cell nucleus in response to oxidative stress (data not shown). However, we have not yet explored the possible contribution of the functional interaction between p53 and GSK3β to the oxidative stress-induced apoptotic response in Huh6 cells.

Taken together, our present findings suggest that, in addition to β-catenin mutation, the abnormal cytoplasmic